2018

Analysis of partial discharge characteristics in insulated twisted pair wires

Sri Surya Shankar Neerukonda

Recommended Citation

ANALYSIS OF PARTIAL DISCHARGE CHARACTERISTICS IN INSULATED TWISTED PAIR WIRES

by

SRI SURYA SHANKAR NEERUKONDA

A THESIS

Submitted in partial fulfillment of the requirements for the degree of Master of Science in Engineering

in

The Department of Electrical and Computer Engineering

to

The School of Graduate Studies

of

The University of Alabama in Huntsville

HUNTSVILLE, ALABAMA

2018

I am presenting this thesis in partial fulfillment of the requirements for a master's degree from The University of Alabama in Huntsville; I agree that the Library of this University shall make it freely available for inspection. I further agree that permission for extensive copying for scholarly purposes may be granted by my advisor or, in his absence, by the Chair of the Department or the Dean of the School of Graduate Studies. It is also understood that due recognition shall be given to me and to The University of Alabama in Huntsville in any scholarly use which may be made of any material in this thesis.
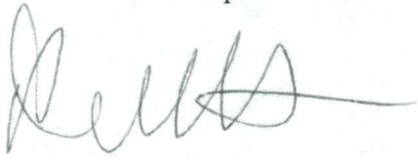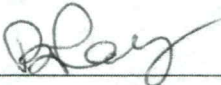
N. S. S. Shankar   12/19/18
_____   _____
Sri Surya Shankar Neerukonda   (Date)
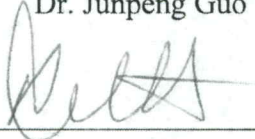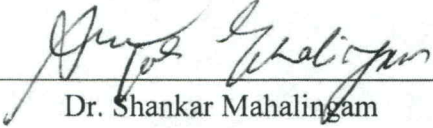
THESIS APPROVAL FORM

Submitted by SRI SURYA SHANKAR NEERUKONDA in partial fulfillment of the requirements for the degree of Master of Science in Engineering in Electrical Engineering and accepted on behalf of the Faculty of the School of Graduate Studies by the thesis committee.

We, the undersigned members of the Graduate Faculty of the University of Alabama in Huntsville, certify that we have advised and supervised the candidate of the work described in this thesis. We further certify that we have reviewed the thesis manuscript and approve it in partial fulfillment of the requirements for the degree of Master of Science in Electrical Engineering.

_____ _____ Committee Chair
Dr. Ravi Gorur   (Date)

_____ _____ Committee member
Dr. Biswajit Ray   (Date)

_____ _____ Committee member
Dr. Junpeng Guo   (Date)

_____ _____ Department Chair
Dr. Ravi Gorur   (Date)

_____ _____ College Dean
Dr. Shankar Mahalingam   (Date)

_____ _____ Graduate Dean
Dr. David Berkowitz   (Date)

iii

ABSTRACT

School of Graduate Studies
The University of Alabama in Huntsville

Degree Masters of Science College/Dept. Electrical and Computer

In Engineering Engineering

Name of Candidate NEERUKONDA SRI SURYA SHANKAR

Title Analysis of Partial Discharge Characteristics in the Insulated Twisted Pair Wires

Due to large-scale integration of renewable energy sources into the power grid, there arises a need of different power electronic equipment for better efficiency and enhanced control. In industries, the most commonly used electric equipment is the motor, more specifically induction motor due to its robust, reliable, efficient and economical operation. Induction motor speed can be controlled efficiently through power converters which are also referred to as adjustable speed drives (ASD). In applications where power electronic converters are deployed, the voltage is in the form of fast switching repetitive pulses. Such conditions are the leading cause of the inception and development of partial discharges in motor insulation. The main objective of this work is to predict and characterize the partial discharge (PD) patterns under the effect of square voltage waveforms. This work presents the dependence of PD characteristics of enamel wires on rise time, pulse width and frequency of the square voltage waveform. These are the primary voltage characteristics which affect the lifetime of the enamel coating. The mechanism of discharges is explained by electric field measurement and space charge model. Results show that the lifetime of the sample is affected considerably by space charge accumulation. This accumulation of space charge modifies the electric field in the air gap of the

iv

twisted pair enamel wires and influences the partial discharge inception voltage (PDIV), leading to degradation of insulation.
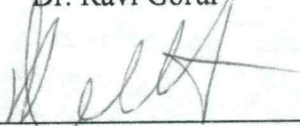
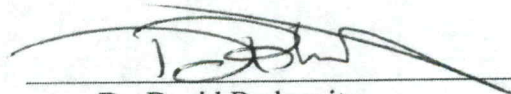Abstract Approval: Committee Chair

_____

Dr. Ravi Gorur

Department Chair

_____

Dr. Ravi Gorur

Graduate Dean

_____

Dr. David Berkowitz

ACKNOWLEDGMENTS

I want to thank everyone who helped me in the completion of this thesis. I firstly thank the almighty for giving me the strength to complete this thesis.

I would like to express my gratitude to my advisor Dr. Ravi Gorur for his patience and immense knowledge and who has inspired me continuously during these two years with his intellectual guidance and constant motivation.

I want to thank my committee members Dr. Junpeng Guo and Dr. Biswajit Ray for their valuable time and suggestions.

I would also like to thank Dr. Yuri Shtessel for his informative ideas and suggestions in framing my work.

I would also like to thank my labmates and friends who supported me throughout my graduation at The University of Alabama in Huntsville.

Finally, I would like to express my profound gratitude to my parents N. V. Rama Rao and N. Sri Lakshmi, my brother N. Kishore Kumar for their spiritual support all the time.

TABLE OF CONTENTS

LIST OF FIGURES

LIST OF TABLES

LIST OF SYMBOLS AND ACRONYMS

PD   Partial discharge

PDIV   Partial discharge inception voltage

SNR   Signal-to-noise ratio

ASD   Adjustable speed drive

IGBT   Insulated gate bipolar transistor

HFCT   High-frequency current transformer

ITSM   Impulsive test synchronization module

BD   Breakdown

EUT   Equipment under test

IEC   International electro-technical council

CHAPTER 1

INTRODUCTION

The ac induction motor is the most prevalent motor technology in application today, constituting more than 90 percent of installed motor capacity. A combination of an adjustable speed drive (ASD) with induction motor results in a high efficiency system, which can cover a wide range of applications. Due to their excellent efficiency, reliability, process precision, improved power factor and inherent flexibility for controlling industrial processes, these converters were in a great demand. The developments in converter technology allowed in reduction of switching loss and improved stability of motor torque. However, the applied voltages contain high-frequency harmonics (distorted voltages) thereby putting winding insulation of electric equipment at risk of failure.

It has been observed that implementation of ASD has worsened the performance of electric motors deteriorating the insulation of motors [27]. They have a detrimental effect on the insulation life and efficiency of motors. The continuous exposure of insulation systems to the distorted voltages increases the risk of enhanced partial discharge (PD) activity and space charge accumulation, thus causing accelerated aging and premature failure [6].

According to IEC 60270 standards, Partial discharge can be defined as

"A localized electric discharge that only partially bridges the insulation between conductors and which may or may not occur adjacent to a conductor."

It can also be defined as, "Partial discharge is the localized intermittent discharge resulting from transient gaseous ionization in an insulation system where the voltage stress levels have exceeded a critical value."

The primary cause of winding insulation deterioration is because of an increase in PD activity due to electric stress caused by pulse-like waveforms. This electrical stress is caused mainly due to two reasons. First, there is an impedance mismatch between inverter, cable, and motor affecting supply waveform producing ringing and overshoot at the motor terminals. These ringing and overshoot increase with an increase in cable length and voltage slew rate (kV/μs) [1]. Secondly, the square waveforms applied to the motor terminals are not distributed evenly along the whole motor winding, and most of the voltage drop is concentrated on the first few turns of the winding. In the case of random wound motors, the interturn stress due to square voltage waveforms can be significantly high compared to sinusoidal waveforms. Therefore, overvoltages and increased interturn stress can trigger PD activity if partial discharge inception voltage (PDIV) is exceeded.

The objective of this work is to determine the partial discharge characteristics of enamel wire insulation. Though the literature on this topic is quite vast, research is going on actively since the past work is lacking in information about the explanations of degradation mechanisms which will help to improve insulation system endurance to distorted supply waveforms.

After thoroughly analyzing the square voltage waveforms and by changing different parameters of the square waveform, the effect of partial discharge activity on the lifetime of the twisted pair samples was investigated. The degradation phenomena are studied in this thesis work through partial discharge measurements and space charge model assumptions.

1.1 Literature Review and Theoretical Background

The fast-changing repetitive voltage pulses from converters can accelerate insulation aging in inverter-fed motors [16], [21]. Many premature insulation failures were reported in recent decades [21]. When a high voltage square waveform is applied to motor windings, the partial discharge often generates in motor windings. An impedance mismatch between the motor and connection cable which results in inverter surge voltage when the pulse voltage is applied to it. Since the pulse voltage sometimes becomes twice of the applied voltage, partial discharge is often induced by the surge. Therefore, overvoltages and increased interturn stress can trigger PD activity if partial discharge inception voltage (PDIV) is exceeded. When the electrical field in some parts of the insulation is higher than the PDIV, PD activities will happen with high probability, and this is recognized as a principal cause of premature failure of motor insulation.

As for motor windings, the influence of deterioration due to partial discharges is considered as one of the life determination factors of motors. To address this problem, International Electrotechnical Commission (IEC) has released the standards, IEC 60034-18-41 and IEC 60034-18-42, for low voltage motor (Type I: organic insulation) and the high voltage motor (Type II: organic/inorganic insulation), respectively [6]. In Type I insulation systems for low voltage motors, PDIV is tested to ensure that the inception voltage is higher than the voltage output by the converter to avoid PD activities when fed by converters. For Type II insulation, accelerated life tests described in IEC 60034-18-42 can provide lifelines which, in comparison with known lifelines of reference materials, would allow an appropriate electro-thermal insulation design to be performed [45]. However, compared with PD measurement technologies and instruments widely used under sinusoidal voltage, there are many issues which should be re-considered when performing PD tests under repetitive square wave voltages [12].

In this work, PD test systems were set up resorting to ultrahigh frequency (UHF) technology and can be used for both sinusoidal and square wave voltages. A large number of PDIV and endurance tests were carried out on twisted enamel wire samples. Experimental results show that PD characteristics and lifetime results are significantly different under sinusoidal and repetitive square wave voltages, even with the same peak-to-peak voltage and frequency. When performing PDIV and life tests on insulation systems of inverter-fed motors, it is recommended to use repetitive square waveforms. The influence of square voltage waveform parameters on PD and insulation lifetime should also be carefully considered.

When the partial discharge occurs, the surface of the insulating layer of the motor winding is partially eroded. If unattended and not taken care of, degradation of the insulating material by this erosion may induce a fatal breakdown in the cover insulating material. According to a study related to the partial discharge [24], a decrease of PDIV (Partial Discharge Inception Voltage) is strangely affected by a space charge accumulation in the insulating layer. The space charge accumulation is often observed phenomenon when a high voltage is applied to polymeric materials [31]. Only a few studies about the space charge accumulation characteristic in the insulating layer of the windings have been carried out in the past. In this work, a relation has been established between PDIV, space charge accumulation and the electric field in the air gap.

CHAPTER 2

EXPERIMENTAL SETUP AND PROCEDURES

2.1   Overview

During the operation of the inverter-fed motors, motor insulation system experiences fast-changing repetitive pulse voltages generated from impedance mismatch between the motor, connection cable, and inverter. Since the pulse voltage sometimes becomes twice of the applied voltage, partial discharge is often induced by the surge. When the electrical field in some parts of the insulation is higher than partial discharge inception voltage (PDIV), PD activities will happen with high probability, and this is recognized as a principal cause of premature failure of motor insulation.

2.2   Equipment Used for the Experiment

In the experiment, Techimp high voltage pulse generator was used to generate square voltage pulses for aging procedures to emulate the real stress experienced in service by insulation systems of inverter-fed motors controlled by Pulse Width Modulation (PWM). The square waveforms can be either bipolar or unipolar. The square waveforms employed here are unipolar.
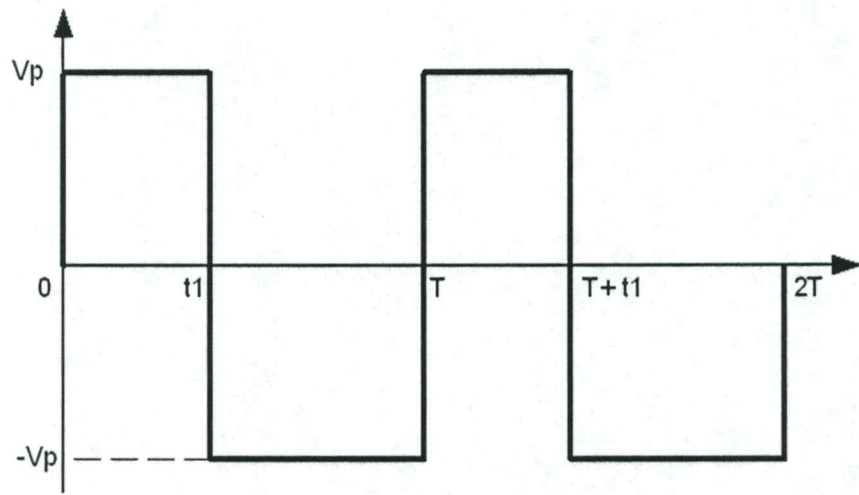
Figure 2.1: Bipolar and Unipolar Square Waveforms
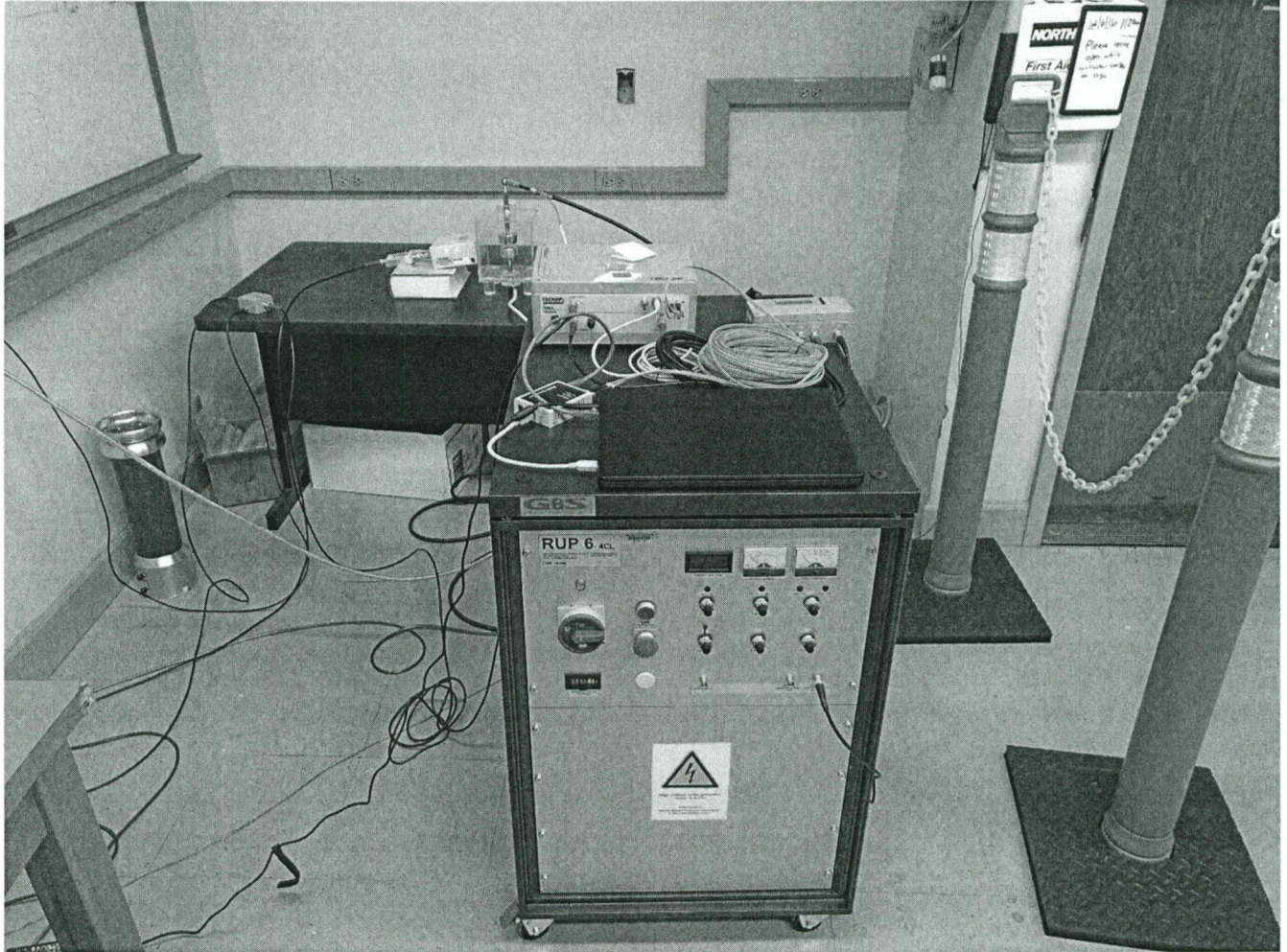
Figure 2.2: Techimp High Voltage Pulse Generator Setup

From the figure, different equipment used in the experiment can be observed. Techimp provides this whole setup. Different apparatus connected will be elaborated in further sections.

2.2.1 Connection Schemes and Circuit Diagram
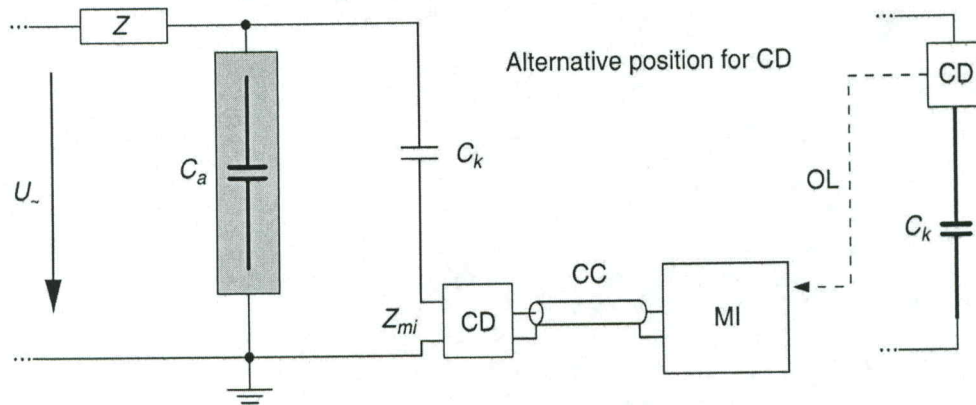
(a) Coupling device CD in series with the coupling capacitor
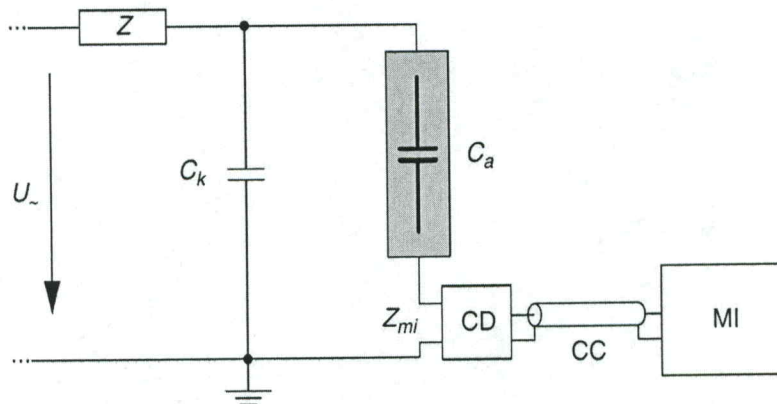
(b) Coupling device CD in series with the test object

$U_\sim$	high-voltage supply
Z_{mi}	input impedance of measuring system
CC	connecting cable
OL	optical link
C_a	test object
C_k	coupling capacitor
CD	coupling device
MI	measuring instrument
Z	filter

Figure 2.3: Circuit Diagram of PD Detection Circuit

This is the conventional PD measurement technique. Figure 2.6 shows a simplified circuit diagram of the PD "straight detection" circuit.

Due to development in semiconductor technology, many companies are manufacturing different measurement equipment with enhanced reliability and to cope up with high voltages. Techimp provides the equipment used in our test setup. Connection schemes are depicted as follows.
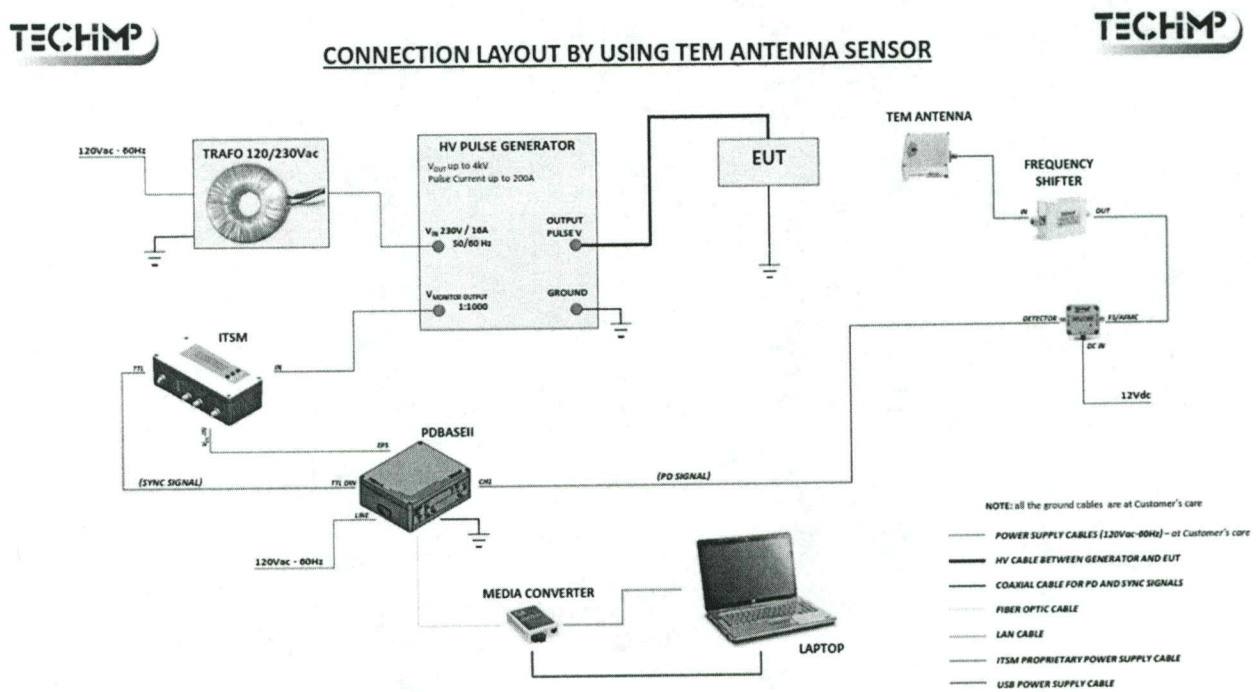
Figure 2.4: Connection Layout by Using TEM Antenna Sensor

The connection scheme in Figure 2.3 is employed to conduct experiments. Here we have different types of equipment namely transformer 120/230 Vac, Techimp high voltage pulse generator, impulsive test synchronization module (ITSM), PDBaseII, media converter, laptop with dedicated software, frequency shifter, detector, and a sensor which is used to detect PD

signals from our sample, equipment under test (EUT). In this connection scheme, we used transmission electron microscopy (TEM) antenna as a sensor. There are two more connection schemes proposed by techimp where clamp high-Frequency current transformer (HFCT) and capacitive divider are used as sensors.

In the further sections, different equipment used in the research and the tasks accomplished by them will be depicted clearly. First, we will discuss techimp high voltage pulse generator. Techimp impulsive voltage testing system exploits techimp state-of-art technology to fully comply the requirements of the IEC 60034-18-41 standard regarding

i). Detecting PD activity,

ii). Measuring PDIV and RPDIV,

iii). Performing the type test on specimens and enamel wires used in the insulation of stator windings.

2.2.2   High Voltage Impulse Generator (RUP6)

The pulse generator RUP6 consists of a number of voltage sources (capacitors), which are charged in parallel with up to 1000V and which are switched in series during the pulse. A specially adapted capacitor charger performs the charging. Depending on the desired output voltage, the modules can be charged up to 1000V. This principle of operation is similar to that of Marx pulse generator. The principle does not request that all modules must be switched synchronously. It's even a unique feature that the modules can be activated sequentially and therefore rise times can be varied over a long range.

A light fiber controls all modules. Malfunction of a module is at first a problem just considering each module itself. So, each module has its own short circuit and arc detection and can autonomously react to overtemperature and overload [51]. Control of the pulse generator (frequency, pulse width, rise/fall time, overshoot, amplitude) is possible by the dials on the front panel. Alternatively, pulse width and frequency can be set by an external logic signal (0V/+5V). To reduce switching losses and to smooth the output signal, the pulse generator has an internal inductor in the output. Its value is 10µH for RUP6 - 4CL.

The principle scheme of RUP6 generator is shown below. The capacitors (180 µF) shown in the Figure 2.7 are charged in parallel using diodes when charging switches (IGBT's) are on. Then after some time the capacitors are discharged in series with the help of discharging switches, thereby delivering 'n' times (if there are n modules) the maximum charging voltage to the load. High voltage IGBT switches are selected for handling high voltage and high frequency as well as their small ON-state voltage drop. Both charging and discharging switches must be capable of withstanding the entire voltage of a single module. Each switch has an isolated driver circuit, which takes its fire command from a controller circuit using a fiber optic link as shown in the Figure 2.7.
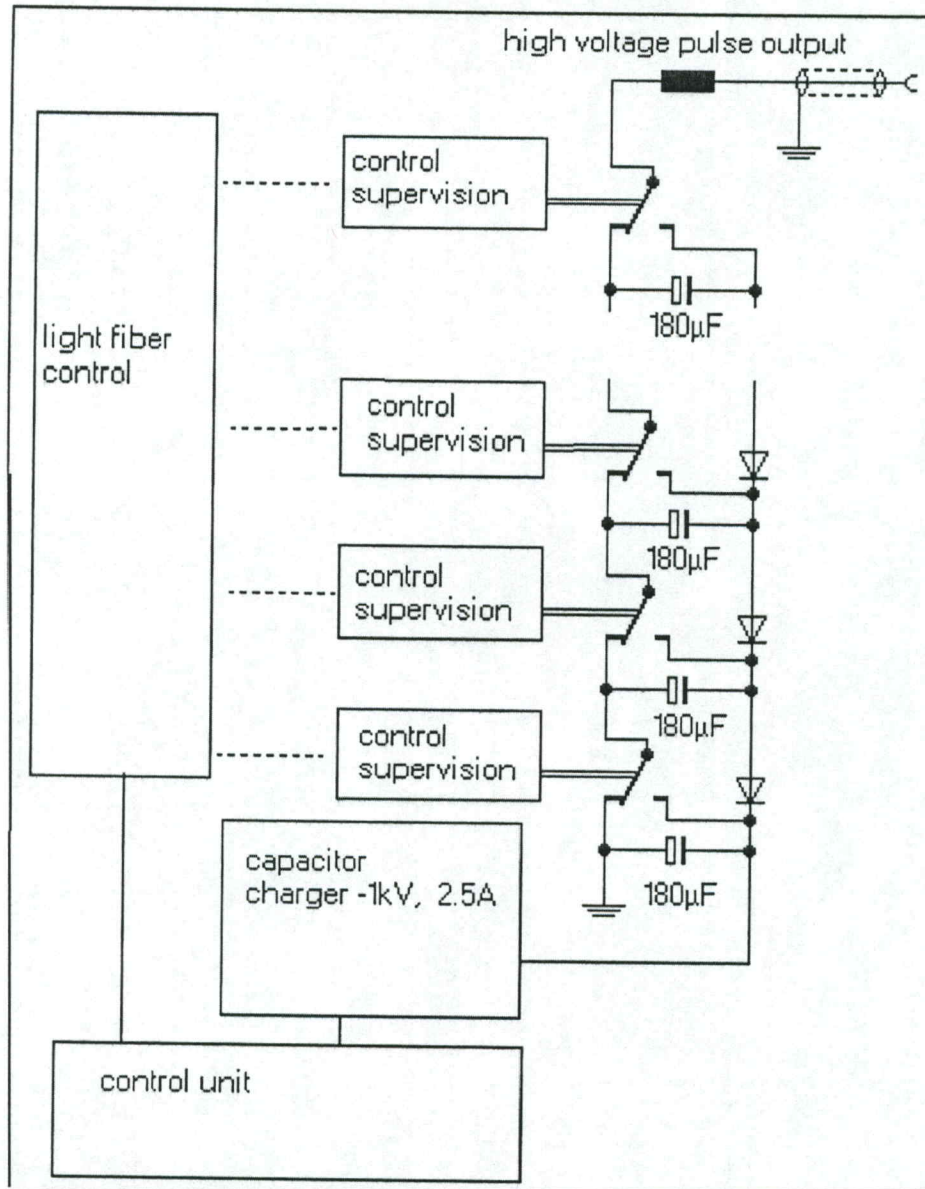
Figure 2.5: Principle Scheme of RUP6 Generator

2.2.3 Partial Discharge Acquisition Unit (PDBaseII)

An innovative instrument for partial discharge recording and processing equipped with fast integrating capability. PDBaseII has been efficiently designed as a system able to collect a large number of PD pulses and separate them according to their waveform. To accomplish this

task, PDBaseII hardware is equipped with an ultrawideband digitizer and integrated processing capabilities. Its fast sampling rate (200MS/s) and its onboard processing capabilities enable us to analyze a considerable number of digitized PD pulse waveforms and pulse features are stored for further processing. There are up to 6 PD channels through which PD signal is received from the sensor, and a dedicated software will be able to perform analysis of the acquired PD signals. The PD signals can be measured both under sinusoidal and impulsive voltages. With the help of this software, PD activity can be monitored continuously, and online monitoring is possible. The internal circuit of PDBaseII is depicted in the Figure 2.8.
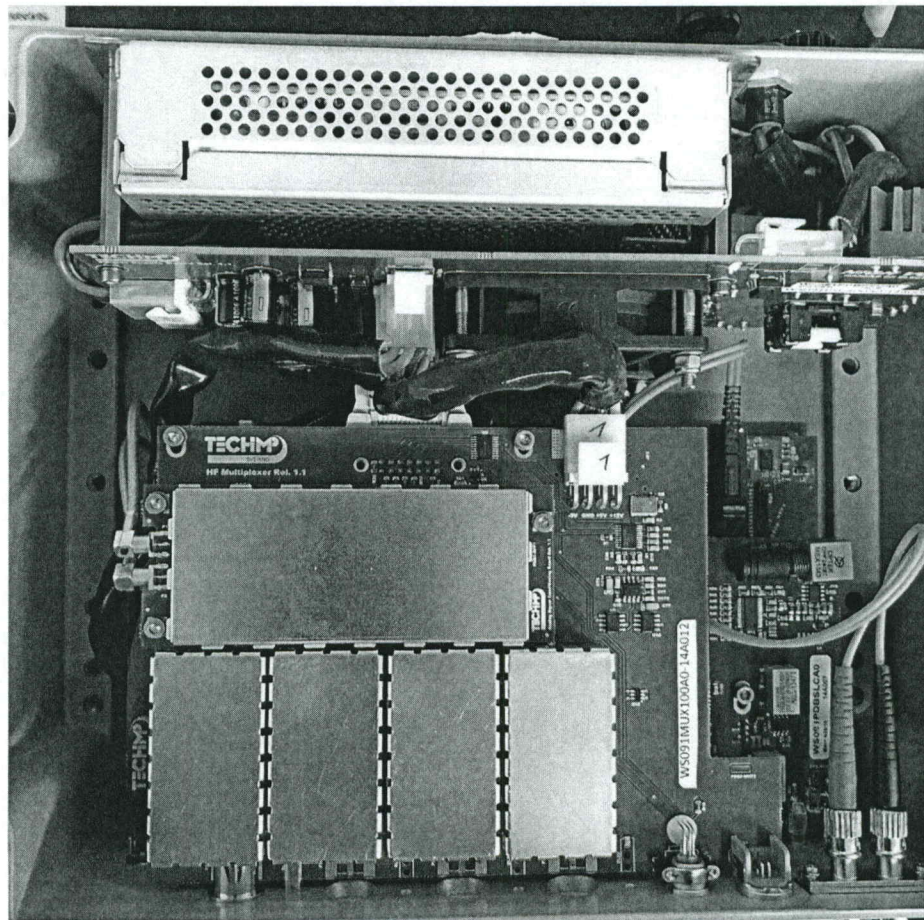
Figure 2.6: PDBaseII with 1 PD channel (top view)

13
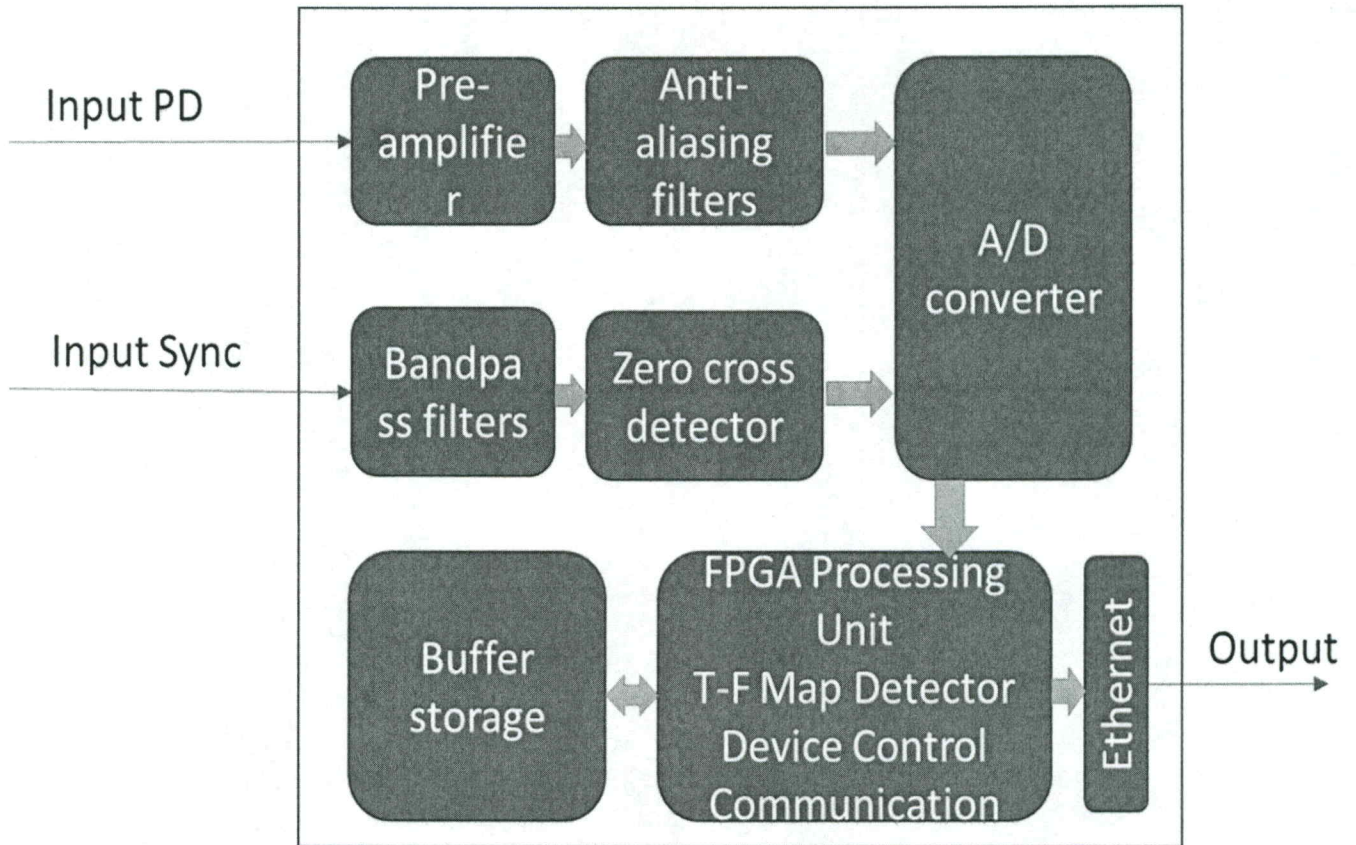
Figure 2.7: PDBaseII Internal Circuit Diagram

2.2.4 Sensors for PD Detection and Synchronization

A UHF antenna is used to detect PD signals owing to its high Signal to Noise Ratio (SNR) and thereby we can reduce the interference of commutation noise generated by the impulse generator with PD pulses. Figure 2.9 shows the sensors.

2.2.5 Frequency Shifter

Frequency shifter converts acquired UHF PD signals into low-frequency signals of the PD detector (below 50 MHz). Frequency shifter is connected between the sensor and the PD

detector. High pass filters are also used in frequency shifter to enhance the signal to noise ratio (SNR). It is shown in the below picture.
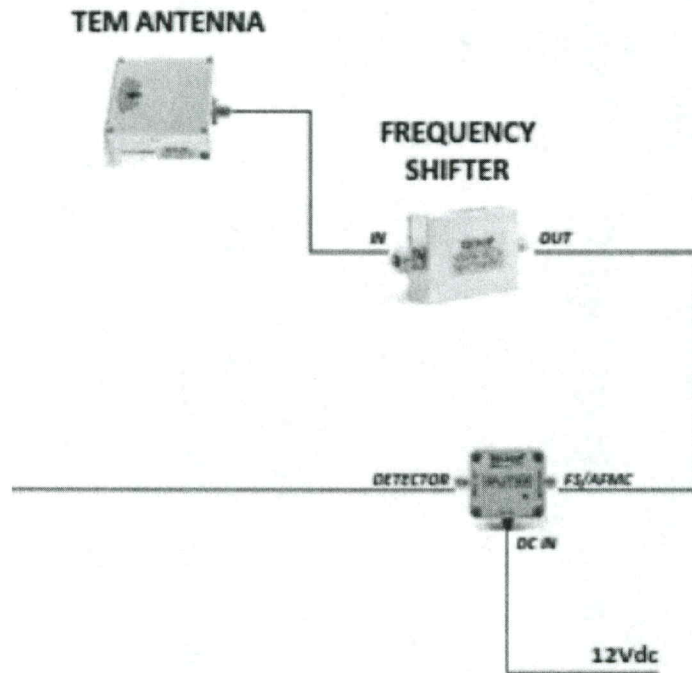
Figure 2.8: Antenna Sensor and Frequency Shifter

2.2.6   Synchronization Block (ITSM)

The impulsive test synchronization module (ITSM) is a device aimed at generating digital synchronization signal which makes PD detection unit able to perform impulsive PD tests. The digital signal generated is synchronized to the voltage impulse of the impulsive source (voltage generator). The ITSM must be connected between the DIN channel of PDBaseII and the output of the synchronization sensor (e.g., capacitive coupler). The ITSM also provides a low voltage signal reproducing the impulsive voltage source.
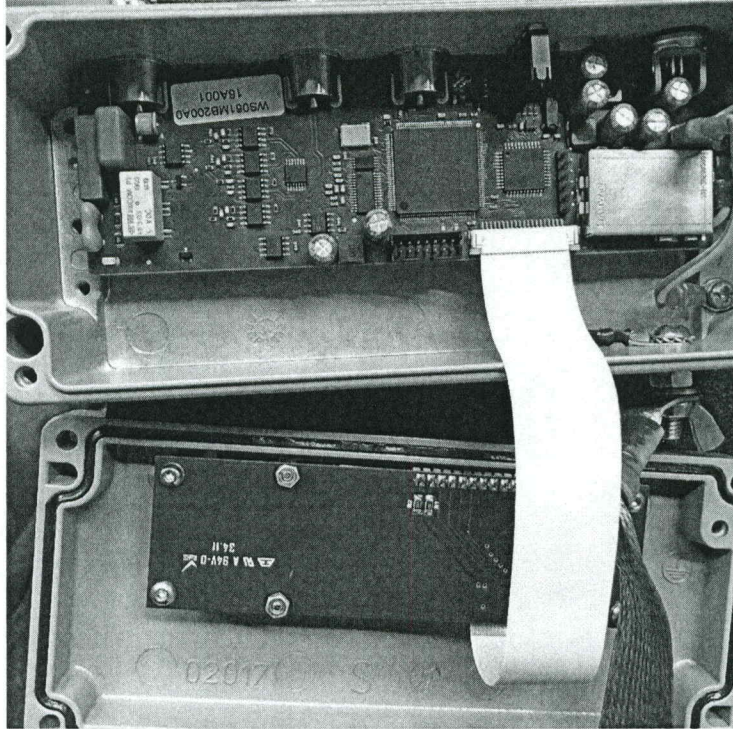
Figure 2.9: Impulsive Test Synchronization Module (ITSM)
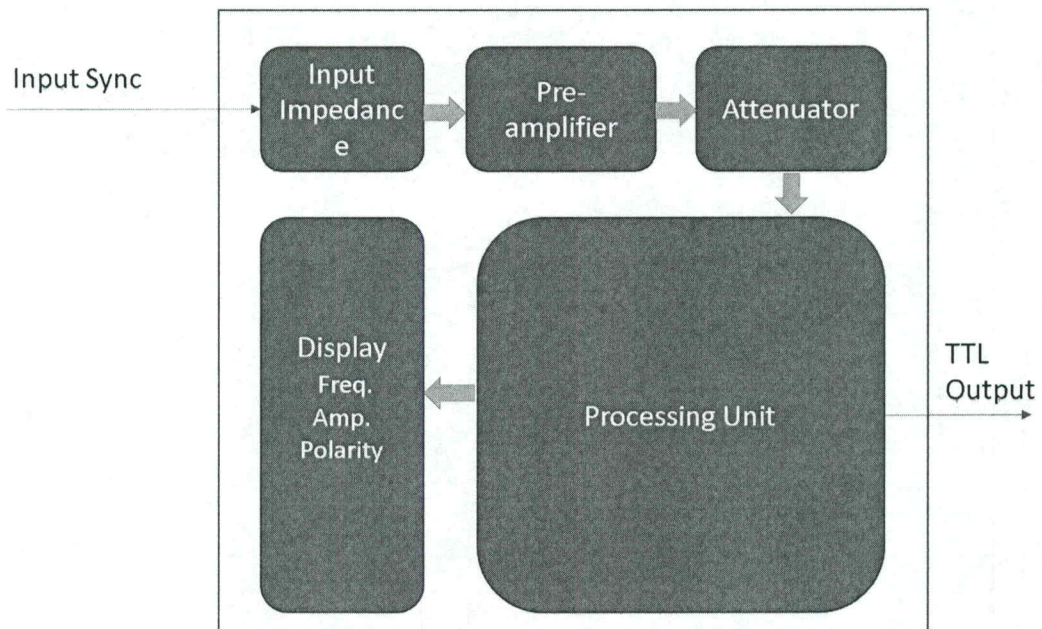
Figure 2.10: Internal Process Flow of ITSM

2.2.7   Analysis and Communication System

The acquired data can be analyzed by connecting a Personal computer to the PD detection unit using fiber optic communication and using a media converter as shown in Figure 2.2.

2.3   Experimental Procedures and Samples

The experiments are conducted mostly on the twisted pair of enamel wire samples. The insulation layer is made of polyamide-imide. The twisted pair configuration is employed because of their resemblance with parallel turns in the stator windings. The samples are shown below and are of different thickness 50 μm, 70 μm, 100 μm.
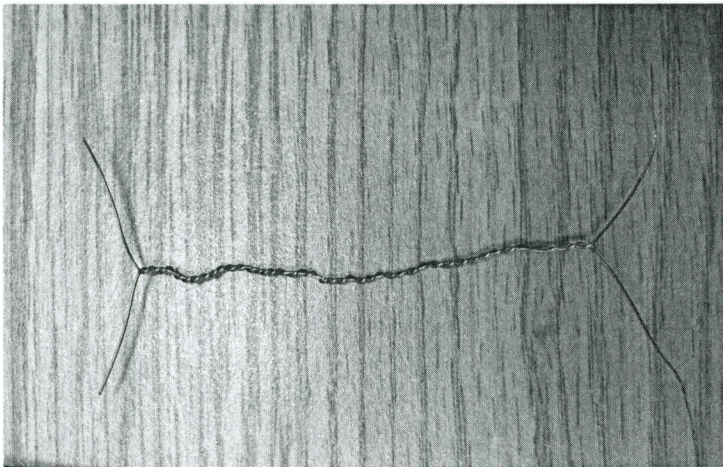
70 μm thickness sample
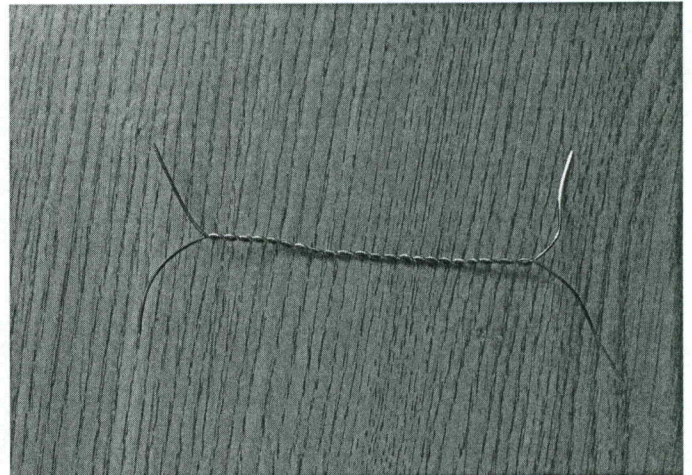
50 μm thickness sample
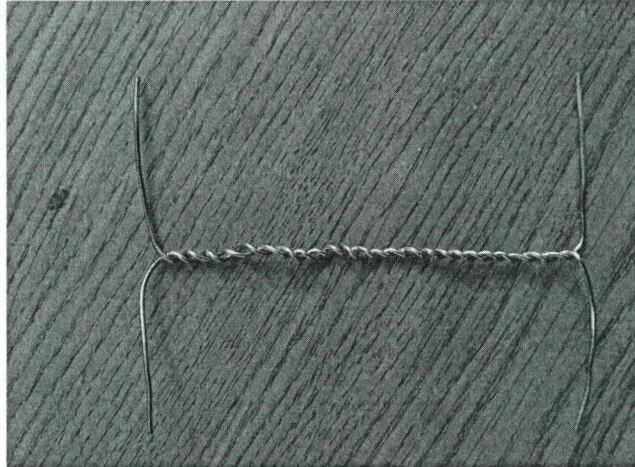
100 μm thickness sample

Figure 2.11: Twisted Pair Enamel Wire Samples

2.3.1 Experimental Procedure

Experimental setup includes a specially designed RUP6 impulse generator by techimp used to produce repetitive square waveforms of different rise times and frequencies. The tests were performed at different frequencies from 100 Hz up to 2000 Hz. For square waveforms, rise times of 300 ns, 2 μs, 5 μs, 10 μs, 20 μs were used. The pulse width of the square waveform can be varied from 0-100 μs, and thereby different duty cycles can be achieved. Various equipment used in the experiment are discussed in the previous sections. In Figure 2.2, connections are depicted.

As shown in Figure 2.2, a 120/230 Vac transformer is used as a supply to the pulse generator. The output of the pulse generator is connected to one terminal of the equipment under test (EUT), and the other terminal is grounded. Regarding experimental procedure, different voltages are applied using the voltage knob on the impulse generator. Generally, we increase

voltage from 0-1000 V at the input, and the impulsive generator is a 4CL generator. So the maximum value of output square voltage pulse is 4 kV. Generally, at the starting, we will begin with low values of voltage and frequency. Then increase the voltage to the desired amplitude, at last frequency to the desired value. When we use the pulse generator for doing long-term insulation stress tests on samples, the generator will, therefore, switch off in case of insulation failure. The operation hours counter can be used to check the time until failure.

After successful connection of all the equipment and when are ready to acquire PD waveforms we must check for a green light on the dedicated PDBaseII software. This work is mostly based on the machine and information obtained from the software.

We have also experimented on some insulation samples other than the enamel wire samples. We used a needle-plane configuration. The different insulation materials used are paper, plastic, filter paper, coated paper, and sandpaper. Experiments are made on these samples to calibrate the machine and to understand the software in detail.

Here is a peek of the streaming window of the PDBaseII software.
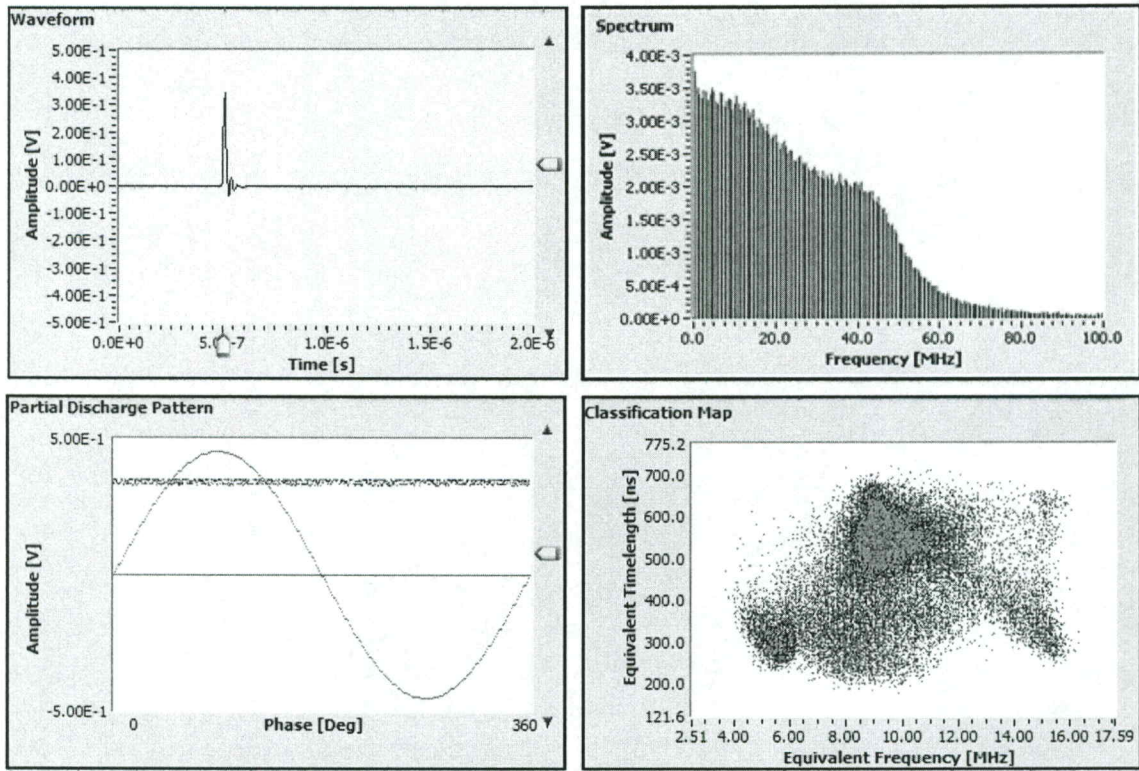
Figure 2.12: Streaming Window Sample in PDBaseII Software

CHAPTER 3

RESULTS AND ANALYSIS

Compared to PD detections at sinusoidal voltages, PD detections under repetitive square voltage waveforms are more complex, since the spectrum of the disturbance produced by the pulse generators might overlap with that of PD pulses. Generally, PD and noise can overlap and then it is almost impossible to distinguish one from the other. Therefore, hardware or software filtering is needed to extract PD pulses from the acquired signals. First, let us discuss various parameters of the square waveform which influences PD characteristics. Based on the past literature [12], the parameters on which square waveform characteristics and ultimately partial discharge characteristics depend upon are rise time, the frequency of the square waveform (SWV), pulse width (duty cycle) and a peak-to-peak voltage of the pulse (V_{P-P}). The partial discharge characteristics also depend upon external parameters like humidity, temperature, etc. The effect of these environmental conditions has been neglected.

3.1 Varying Different Parameters of the Square Wave

The experiments are performed by varying different parameters of the square waveform. The results of plots are discussed in the further sections.

3.1.1 Varying Rise Time

The following observations were obtained by changing the rise time of the pulse maintaining other parameters of the square waveform constant. The frequency is maintained at 2kHz, and the duty cycle is 20%. This is the maximum duty cycle that can be achieved on the

RUP6 pulse generator owing to its low frequency. The pulse peak voltage V_{P-P} is maintained at 2.8kV.

Rise Time (µs)	PDIV (V)	V_{P-P} (kV)	Time to BD (min)	PD Magnitude (V)
0.3	1780	2.8	68	1.3
1	1600	2.8	79	1.3
2	1552	2.8	88	1.2
4	1480	2.8	100	1.1
5	1456	2.8	122	0.8
7	1392	2.8	138	0.7
10	1296	2.8	196	0.3
15	1220	2.8	224	0.3
20	1176	2.8	256	0.2

Table 3.1: Statistics Related to PD Features for Sqaure Waves with 2kHz Frequency and Different Rise Times

From Table 3.1, it can be observed that with an increase in rise time from 300 ns to 20 µs, time to breakdown increases, PD magnitude decreases, and PDIV also decreases with the

increase in rise time. The plot of rise time vs. Time to failure is as shown below.
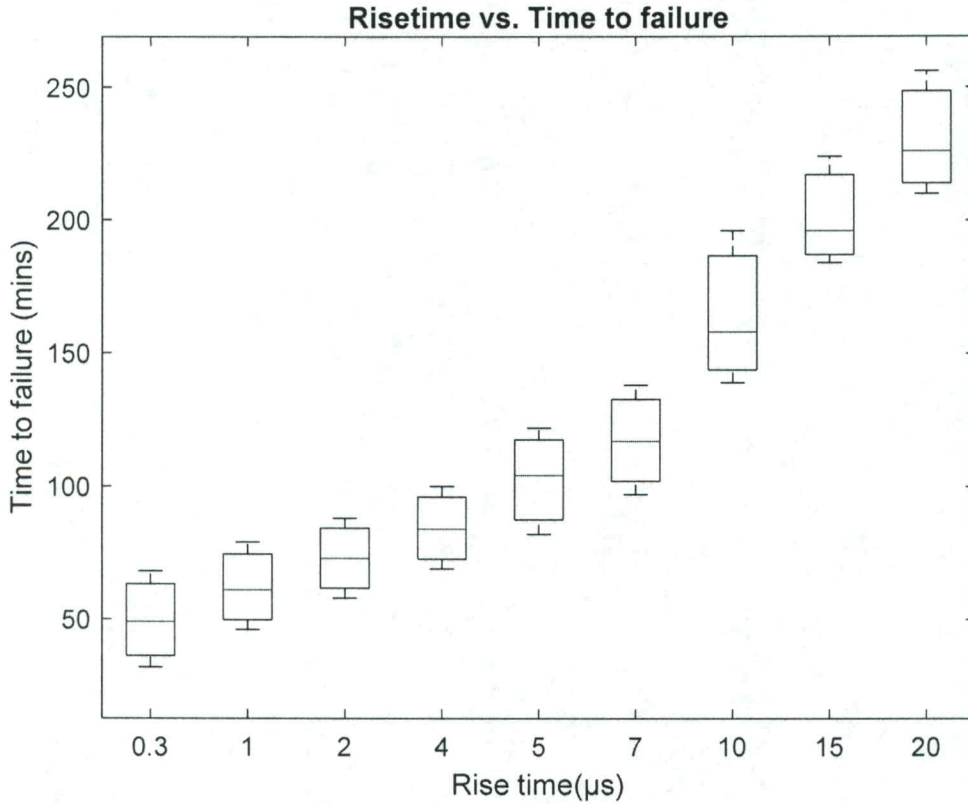
Figure 3.1: Rise Time vs. Time to the Failure of the Samples

Figure 3.1 reports the breakdown times of twisted pair enameled wires under unipolar impulse square waveforms at a frequency of 2 kHz. As observed in Figure 3.1 the average lifetime increases significantly with increasing rise time. The endurance times of square wave voltage at 15 µs rise time and above is around 3-4 times longer than those obtained at square wave voltages with 300 ns rise time. Clearly, the rise times of the impulse waveforms can influence the lives of the crossed pairs significantly.

This behavior of the sample concerning the rise time can be attributed to the fact, at low rise times (rate of rise of the voltage from zero to peak value is high i.e. dv/dt is high), there will

be a huge voltage surge within the sample which creates stress and gives rises to partial discharge. As the rise time increases, the smoothness of the waveform increases and apparently it becomes sinusoidal where the lifetime of the sample is high.
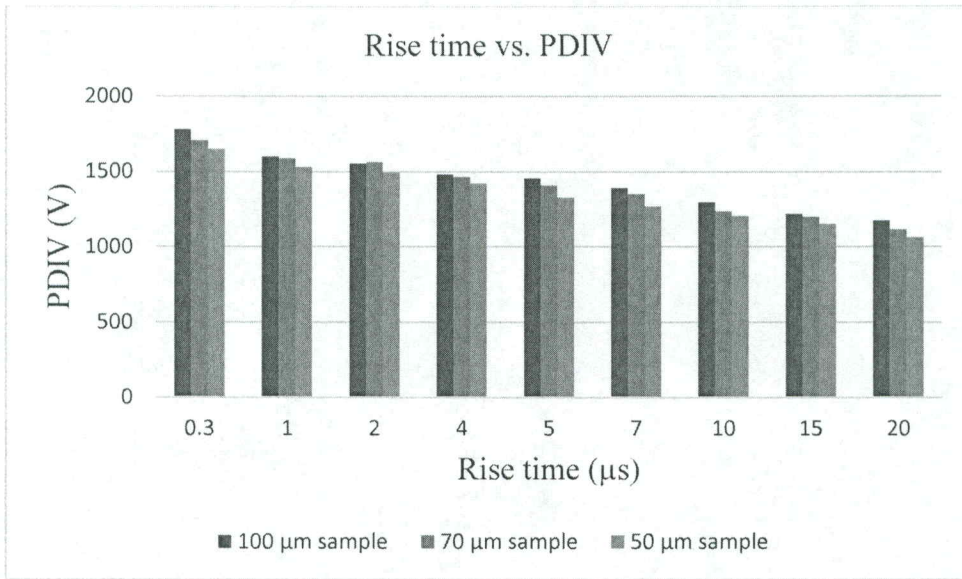
Figure 3.2: PDIV vs. Rise Time

By recording the applied voltage and the PD signal simultaneously, it was possible to observe that, with shorter rise times, PD with large magnitude tend to occur at higher voltage levels (here defined as PD inception voltages). These observations can be explained since a PD can be incepted under following conditions: i) the electric field is sufficiently high, and ii) a starting electron is available to initiate the discharge avalanche. Due to the stochastic nature of starting electrons PD process begins with some delay with respect to the time the field becomes sufficiently high. Therefore, the faster the rate of rise of applied voltage (the shorter rise time), the larger will be the overvoltage at which PDs will occur and it is shown in Figure 3.2.

24
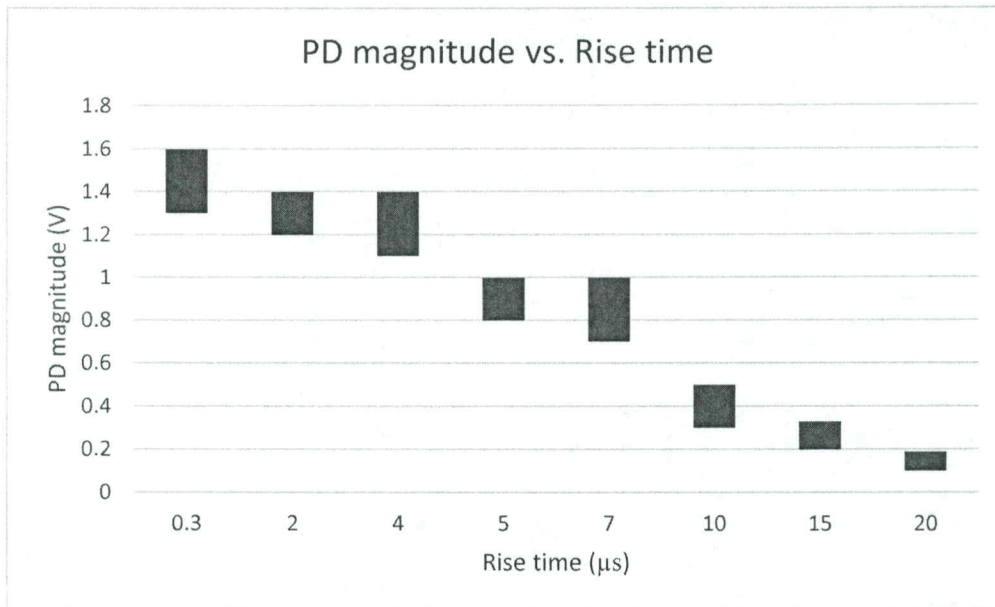
Figure 3.3: PD Magnitude vs. Rise Time

To study the PD features recorded during life test on enamel wires, Figure 3.3 reports the PD magnitude of twisted pair enamel wires versus impulsive voltage rise times at 2 kHz test frequency. In this figure, average PD magnitude increase as rise time decreases. It can explain why lifetime shortens with short impulse rise times since PD is the crucial reason causing insulation degradation.

To study the role of total partial discharge numbers experienced by the twisted pair enamel wires from the beginning of the test to final breakdown on the insulation, the average discharge number to the breakdown was obtained and shown in Figure 3.4. The most interesting observation is that the total discharges experienced by the sample increase with increasing rise time. At rise time of 20 μs, the samples experienced the greatest number of discharges, which is two times more than that of the discharges experienced by the samples at impulse voltages with 300ns rise time. This shows that the total number of discharges might not be the most important factor causing the final insulation breakdown. Alternatively, PD activities with large magnitude could be a more crucial factor causing the insulation breakdown.
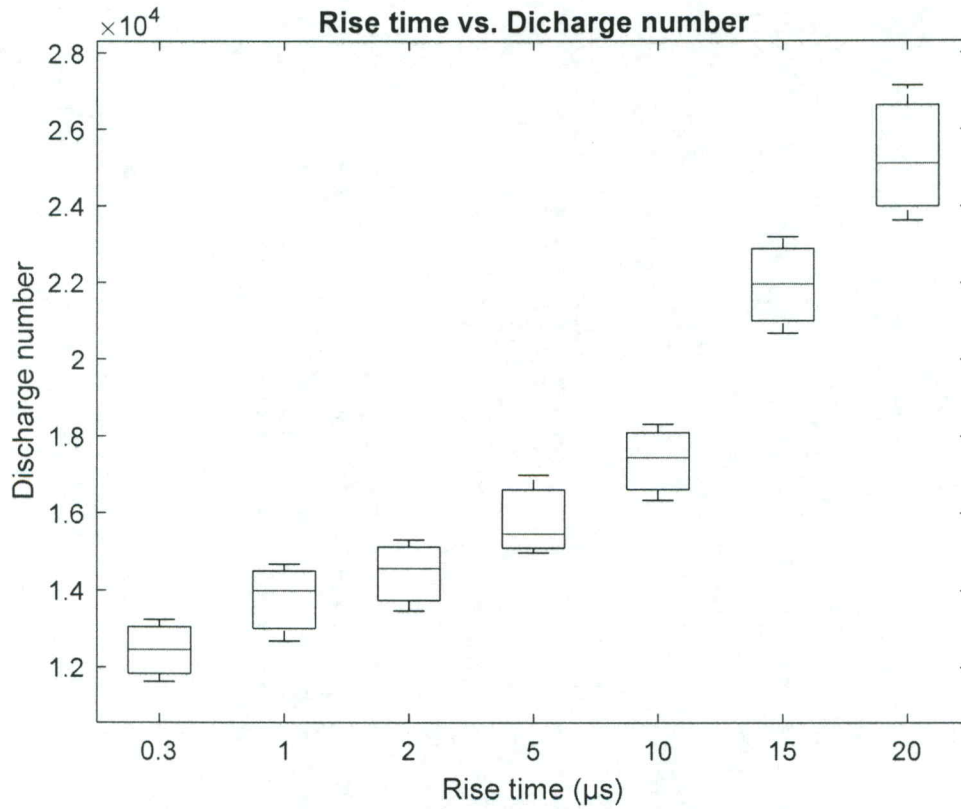
Figure 3.4: Rise Time vs. Discharge Number

3.1.2 Varying Frequency

PD activities for specimens were studied with a rise time of 300 ns at room temperature, with peak-to-peak magnitude of 3 kV, which is higher than partial discharge inception voltage (PDIV) and the duty cycle is 20%. This is the maximum duty cycle that can be achieved on our pulse generator owing to its low frequency. The plot of frequency vs. time to failure of the sample is as shown below. The table below shows the experimental data varying frequency.

Frequency (Hz)	PDIV (V)	V_{P-P} (kV)	Time to BD (min)	PD Mag (V)
100	1764	3.0	264	0.3
500	1788	3.0	224	0.5
750	1784	3.0	208	0.6
1000	1776	3.0	186	0.8
1250	1748	3.0	164	0.9
1500	1756	3.0	148	0.9
1750	1760	3.0	136	0.9
2000	1752	3.0	125	0.9

Table 3.2: Statistics Related to PD Features for Square Waves at Rise Time of 300ns, 20% Duty Cycle and Different Frequencies
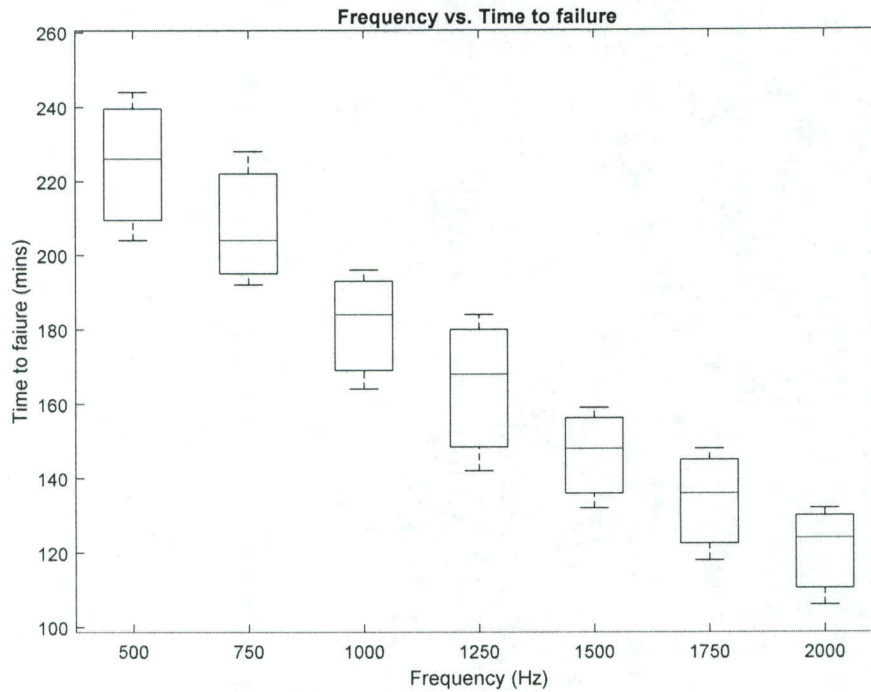
Figure 3.5: Frequency vs. Time to Failure

It was observed that increasing the switching frequency from 0.5 kHz to 2 kHz reduced the time-to-failure by a factor of two (Figure 3.5). This can be attributed to the fact that, with an increase in frequency, the time period of the waveform decreases. Therefore, less time is available for the electrons to recombine, generating more free electrons leading to increase in discharges and hence increase in PD. So, the probability of breakdown is high with an increase in frequency.

From Figure 3.6, it can be observed that PD magnitude increased from 0.5 V to 0.8 V when the switching frequency was increased from 0.5 to 1 kHz, whereas only an increase to 0.9 V occurred when the frequency was further raised to 2 kHz. This means that energy in the PD pulses is extinguishing with increasing frequency and reached saturation beyond 1 kHz. From the experimental data in the above table, we can observe that PDIV is almost independent of

frequency and this is affirmed by Fabiani in his paper[42]. We have performed experiments varying frequency and recording PD amplitude with the discharge patterns obtained from PD BaseII software. The following plot explains the dependency of PD amplitude on frequency.
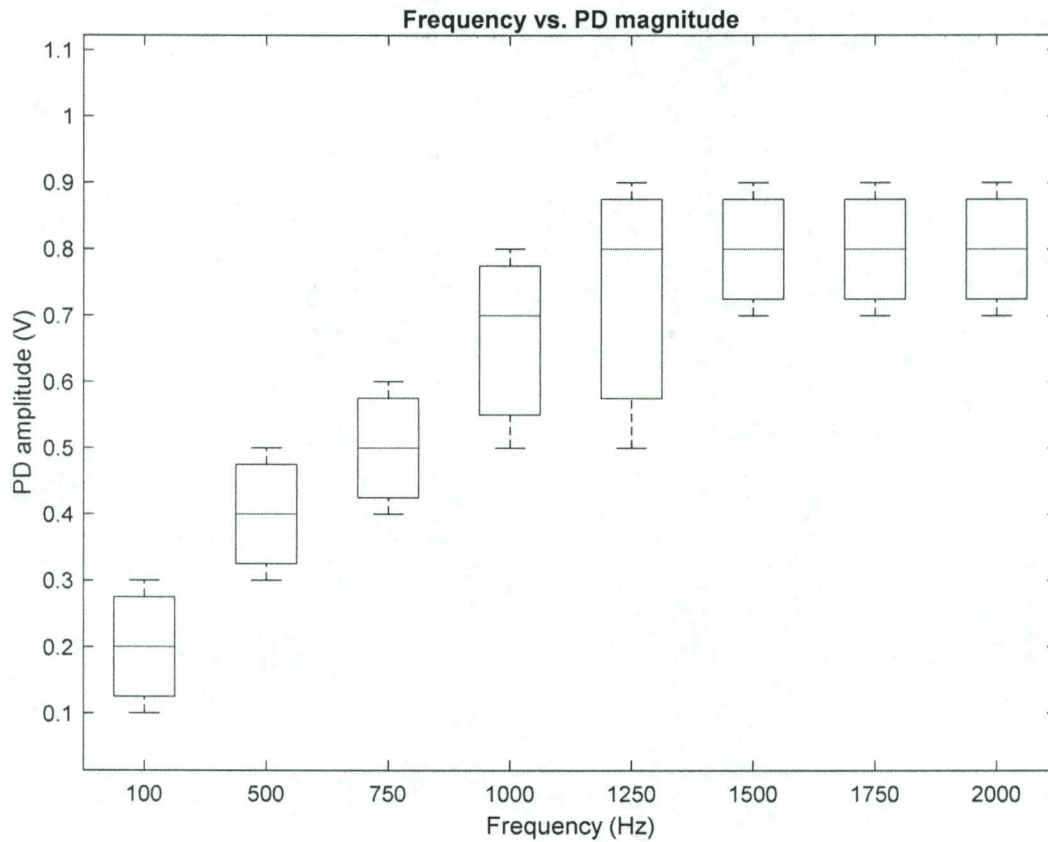
Figure 3.6: Frequency vs. PD Amplitude

From the plot, it can be observed that PD amplitude rises increasing supply frequency (with saturation effect above 1000 Hz). Reductions in PD magnitudes are caused by a reduction in surface charge transfer and may also be due to the mobility of the surface charges on the insulation film. As the switching frequency increases, the time becomes shorter for charge depletion on the insulation film increasing the PD magnitude, thus resulting in a residual charge on the surface that increases with increasing switching frequency. One of the interesting

observations made is that the frequency measurements in this work do not entirely comply with the previous work [33].

3.1.3   Varying Pulse Width

With the applied voltage, switching frequency and rise time kept constant at 3.2 kV, 2 kHz, and 300 ns, respectively, the effect on aging was investigated for duty cycles of 5%, 7.5%, 10%,12.5%, 15%, 17.5% and 20%. Figure 3.7 shows the plot of Pulse width vs. Time to failure of the sample.

Pulse width (µs)	Duty cycle (%)	V_{P-P} (kV)	Time to BD (mins)	PD amplitude (V)
25	5	3.2	254	0.6
37.5	7.5	3.2	186	0.7
50	10	3.2	156	0.9
62.5	12.5	3.2	104	0.9
75	15	3.2	97	1
87.5	17.5	3.2	88	1.1
100	20	3.2	74	1.4

Table 3.3: Statistics Related to PD Features for Square Waves at Rise Time of 300ns, 2 kHz Frequency and Different Duty Cycles.
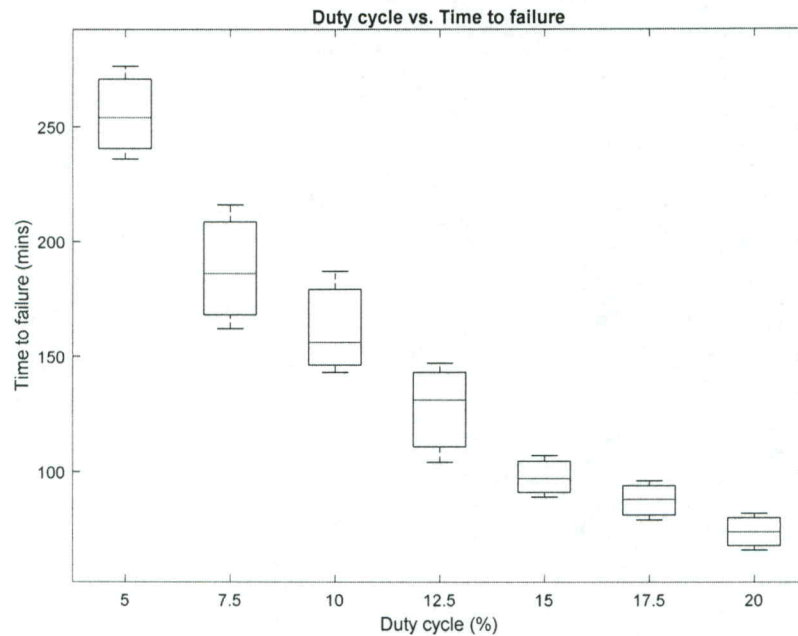
Figure 3.7: Pulse Width Vs. Time to Failure

From the plot, it can be observed that, decreasing the pulse width of the input voltage, i.e., with a reduction in the duty cycle, the lifetime of the enamel wire sample increases. This can be attributed to the fact that, when the duty cycle is more, i.e., ON time of the pulse is more, which means voltage is high for the extended amount of time, so there is a more chance of PD occurrence.

rise time (μs)	Duty cycle (%)	PD amplitude (V)	PD Number
0.3	20	1.4	12168
5	20	1	15133
0.3	5	1.2	8486
5	5	0.6	10589

Table 3.4: Statistics Related to PD Features for Square Waves at 2 kHz Frequency and Applied Voltage of 3.2 kV for Different Rise Times and Duty Cycles

31

To study the effect of both duty cycle and rise time on PD activity, experimental results are depicted in a table. When the duty cycle is reduced from 20% to 5%, the number of occurrences of PD diminishes and this result may be due to the greater relaxation time created by the reduction in the time in which the electric field is present in the insulation. This could lead to a lower accumulation of the space charge, thus causing discharges in the flat portion. In such a case, it is possible to observe the effect of the rise time.

At a fast rise time of 300 ns, due to the presence of the time lag in the formation of the discharge, the electric field exceeds well above the PD threshold before the discharge takes place, generating additional charges. Assuming a similar time lag for slower rise times, the electric field enhancement is lower for a slower rate of rise (low dV/dt) so that a smaller amount of charge is generated. This effect occurs because of the accumulation of greater charges for the pulse with a longer duty cycle, in which case the electric field is present for a longer time. Therefore, as indicated in Table 3.4, the number of PDs increases from 8486 to 12168 when the duty cycle is increased from 5% to 20%. Relating this observation to the results of the time-to-failure tests shown in Figure 3.7, one can say that additional number of PDs with a high PD amplitude can contribute to faster failures, as occurred for 20%, rather than concentrated high amplitude pulses at lower rise time, as occurred for 5%.

It can also be observed that a higher number of PDs as well as the occurrence of PDs in the 'ON' time of the pulse contribute to faster failure. Although accumulated pulses at 5% are present with a high amplitude, failure is faster at 20%, where a greater number of PDs are observed. It can be deduced from this that the number of PDs and the sum of the PD amplitudes represent the total energy delivered to the insulation by the PD, which is related to the failure of the insulation.

32

3.1.4　Life Behavior with Peak-to-Peak Voltage (V_{P-P}):

With the switching frequency, duty cycle, and rise time of 2 kHz, 20%, and 300 ns, respectively, the applied voltage was varied as a means of observing the effect of applied voltage on the times-to-failure (Figure 4.5). The voltage is varied from 1.6kV to 4kV.
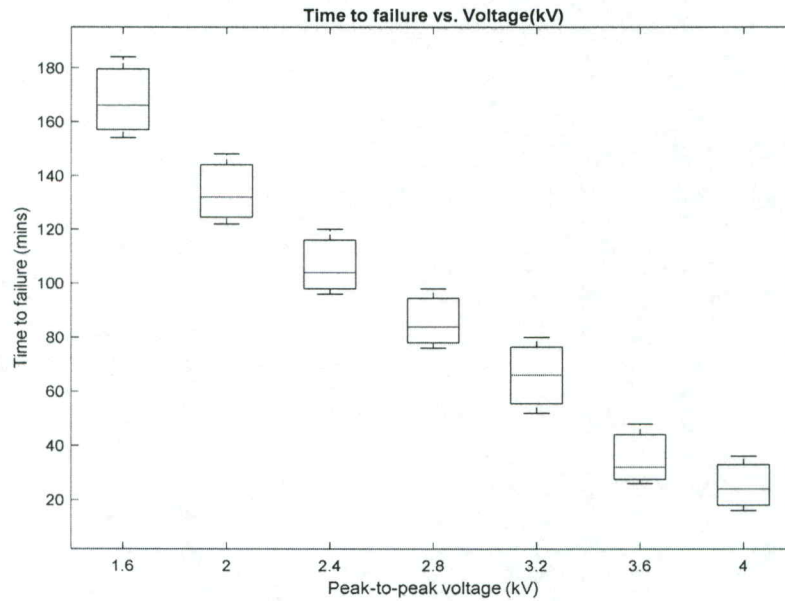
Figure 3.8: Peak Voltage vs. Time to failure

From this plot, we can assess that time to failure of the sample is inversely proportional to the peak-to-peak voltage of the pulse. This outcome means that increasing the applied voltage from 1.6 kV to 4 kV changes the aging mechanisms, possibly due to exceeding the repetitive PDIV threshold.

3.2　Partial Discharge Patterns

Now, let's examine the PD patterns acquired by PDBaseII. These discharge patterns will help us to assess the PD activity over time and with increasing input voltage of the generator.

The PD patterns are collected at regular intervals which enable us to investigate PD variation with time and with the increase in the pulse voltage (V_{P-P}).

3.2.1 Partial Discharge Patterns of 100μm Insulation

After 10 mins

After 30 mins
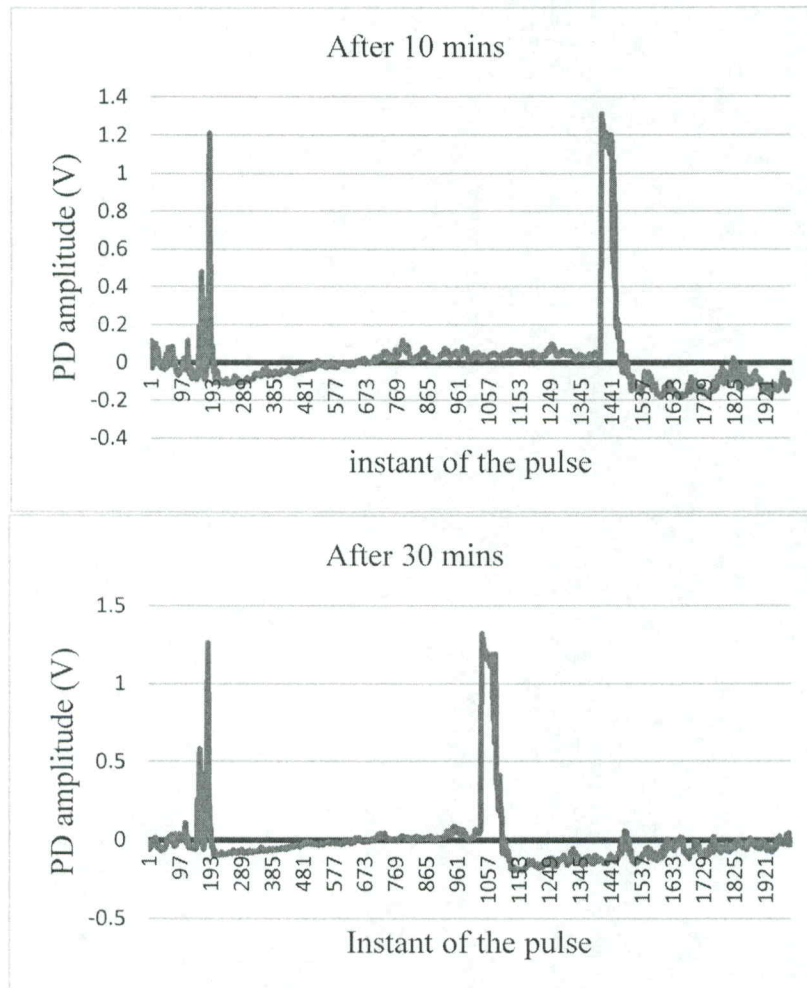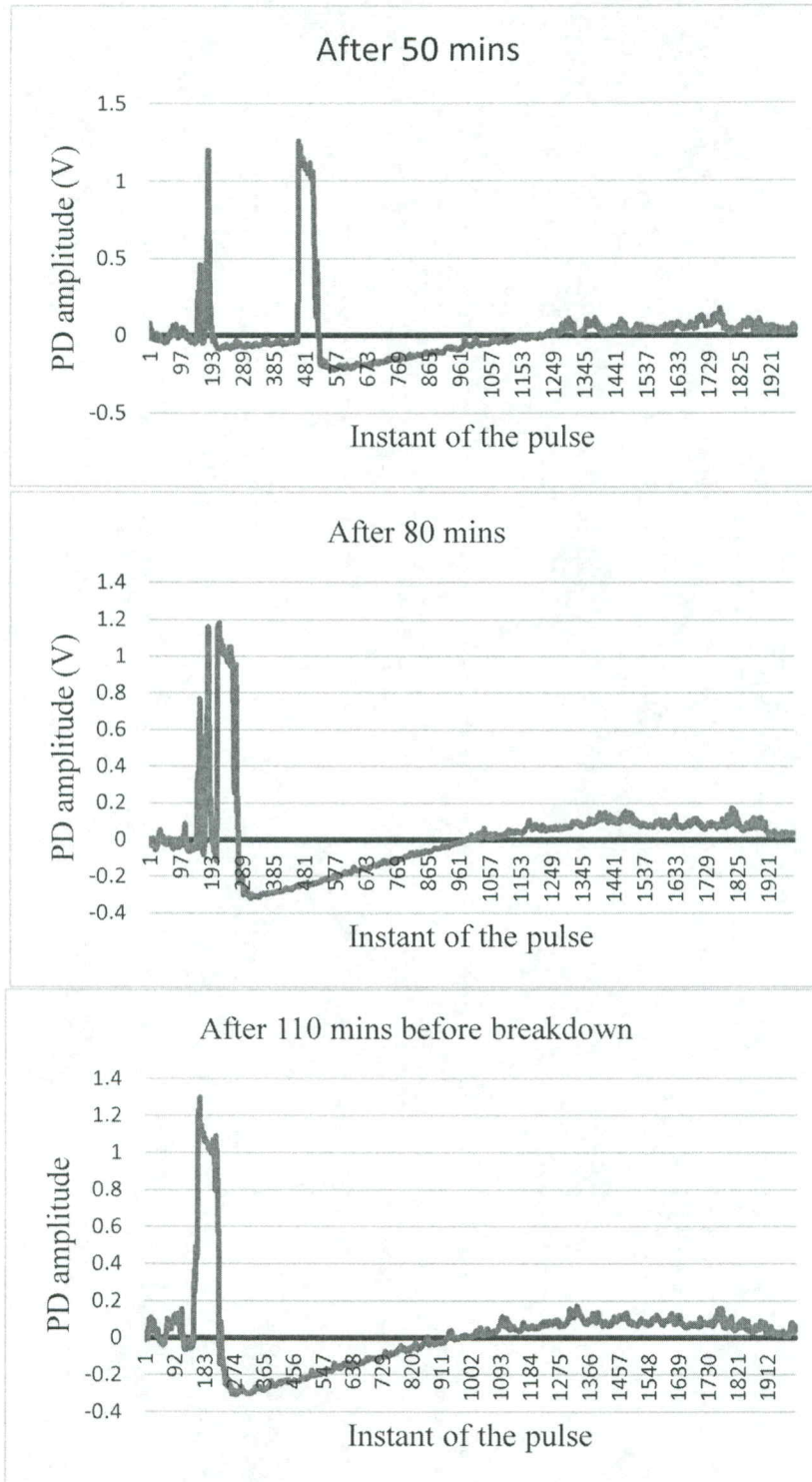
Figure 3.9: Partial Discharge Patterns of 100 μm

From these patterns, we can observe a considerable difference in PD patterns after ten mins and after 80 mins and 110 mins before breakdown. The PD pulse is converging with

commutation pulse generated from the generator over time with an increase in voltage. From the last PD pattern, we can assess that as the voltage increases and over time PD pulse seems to be having more width than typical random and instantaneous pulse. This is because of energy modification around the PD site.
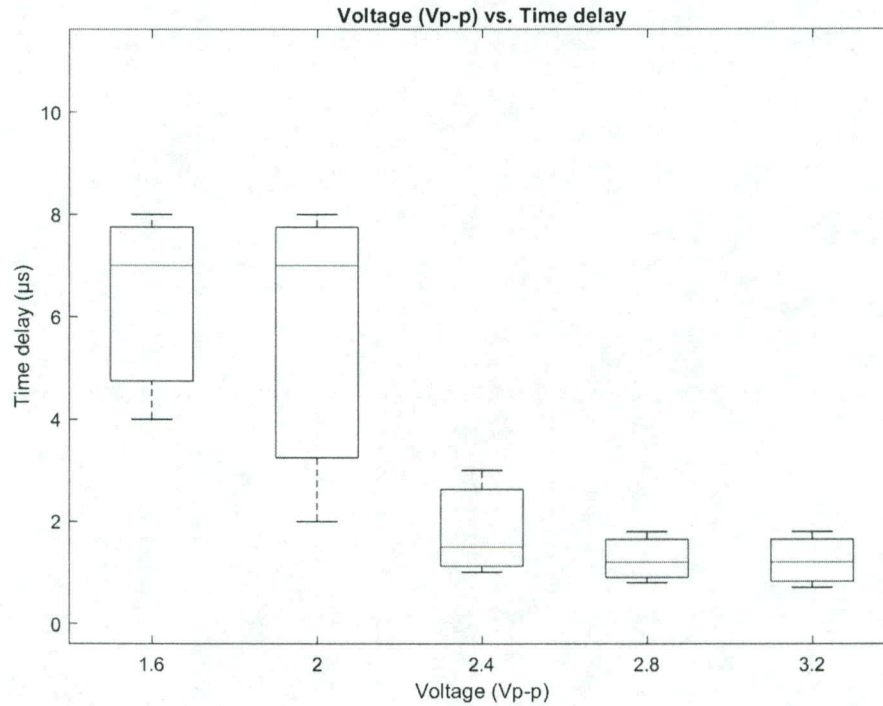
Figure 3.10: Peak-to-Peak voltage (V_{P-P}) vs. Time Delay

From analyzing above patterns, time delay between the commutation pulse and the PD pulse is calculated. This time delay and increase in peak-to-peak voltage (V_{P-P}) are plotted. From this plot we can observe that time delay decreases with increase in peak-to-peak voltage (V_{P-P}). This can be attributed to decrease in statistical time lag (τ_{stat}) of the PD process. Statistical time lag (τ_{stat}) is the time difference between the time when the inception field is exceeded and the occurrence of a PD. τ_{stat} is a result of unavailability of a free electron to initiate a PD after the inception field is exceeded, resulting in a time delay of a PD occurrence. In the last pattern, when

36

the sample is approaching breakdown the τ_{stat} is almost very low such that PD happens very spontaneously and converges with the commutation pulse.

With the help of this equipment and test setup, continuous monitoring of insulation degradation in the motors can be achieved. By analyzing these patterns, the point at which the sample will breakdown can be known, and necessary steps can be taken to prevent premature insulation failure of the system. From these patterns, enough information cannot be obtained on the PD mechanism happening inside the insulation. So, further analysis has been carried out in the following sections.

3.3   Sample Analysis

To understand the cause of insulation degradation with an increase in voltage in the twisted pair enamel wires, average discharge number has been calculated from the PD patterns obtained and their variation in samples of different thickness. The degradation mechanism happening inside the insulation because of the stresses should be analyzed. The possible stresses which lead to degradation are thermal, mechanical and electrical. However, we are concerned only about electrical stress in our work.

When the discharge occurs, it will leave some charges at the discharge site, and the energy released from these charges might make a difference in distinguishing between failed and passed samples. Now we will discuss how the number of PD pulses of samples of different insulation thickness has an impact on the lifetime of the sample which leads to the degradation and breakdown of the sample. First, let us discuss failed samples of different thickness at a peak-to-peak voltage of 3.2 kV.

3.3.1   Failed Samples:

From PD patterns obtained above, data has been collected and exported that data into excel sheet and calculated the number of pulses at regular intervals. Here 1.2 V is taken as reference because the noise pulse generated by the generator is of magnitude 1.2 V. The following plots show how the number of PD pulses increases with increase in voltage over time.
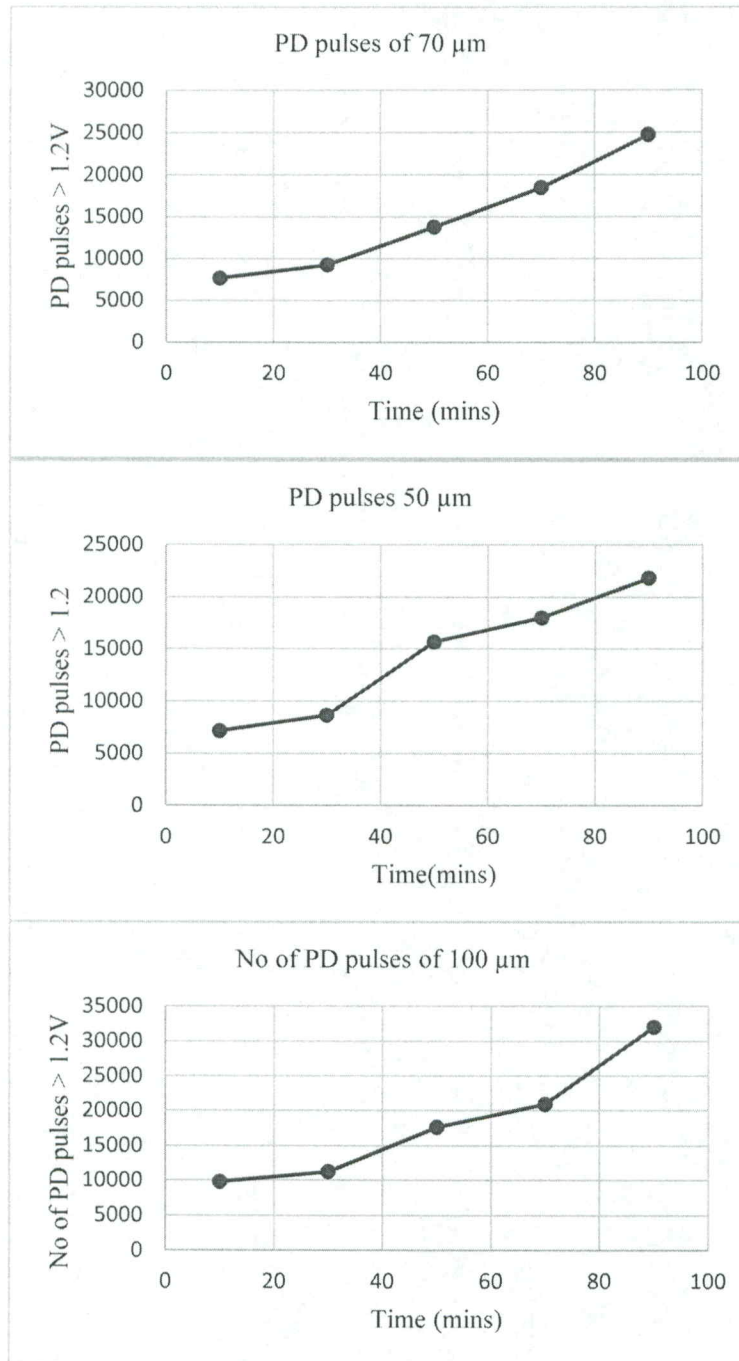
Figure 3.11: Plots of Samples - Number of PD Pulses vs. Time to Failure
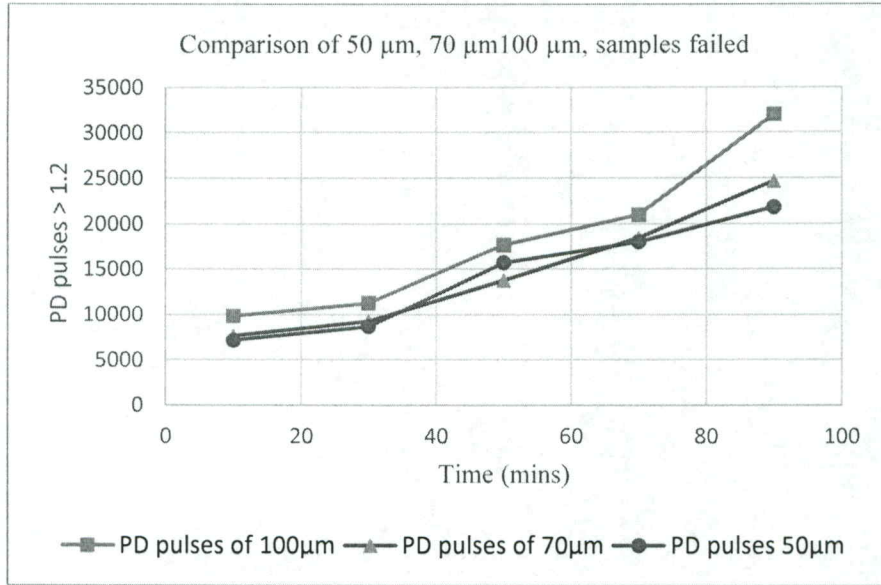
Figure 3.12: Comparison of 50 μm, 70 μm, 100 μm Failed Samples
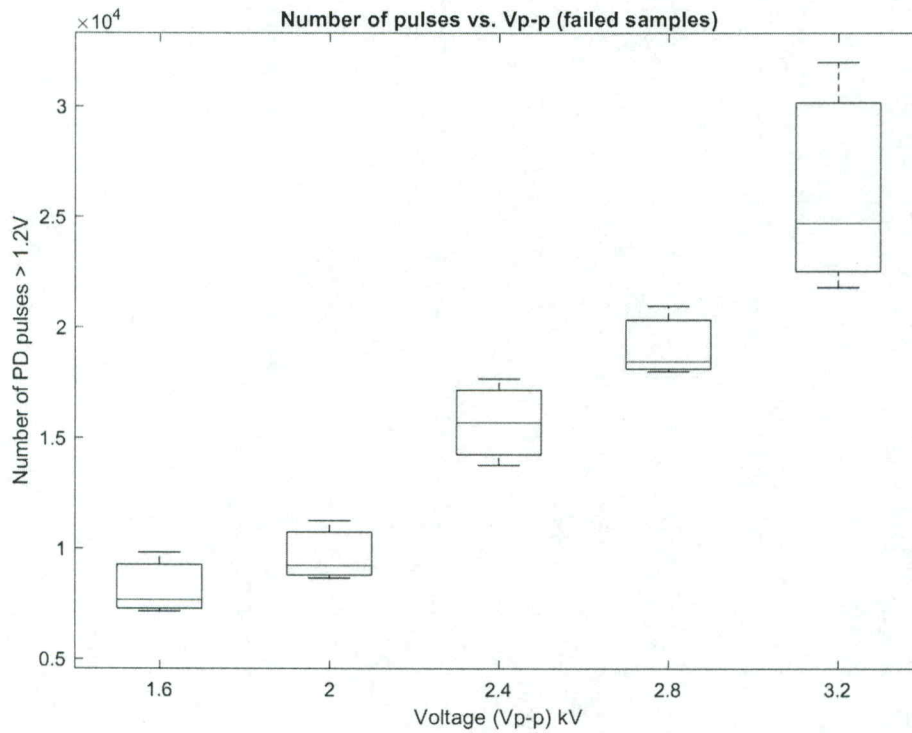
Figure 3.13: Number of PD Pulses > 1.2V vs. Peak-to-Peak Voltage (kV)

From the above plot, it is observed that PD activity increases with an increase in peak-to-peak voltage (V_{P_P}) of the pulse. As the voltage is high, insulation is stressed more due to high electric field in the air gap or void which is far beyond inception voltage. Due to repetitive PD activity, charge has been accumulated in the insulation bulk and in the air gap of the twisted pair enamel wires. The impact of this accumulated charge on electric field in discharge sites of the insulation is studied in the next chapter.

3.3.2 Passed Samples

Some of those samples did not break down and endured for around 4.5 hrs. The peak-peak voltage maintained here is 2.5 kV.
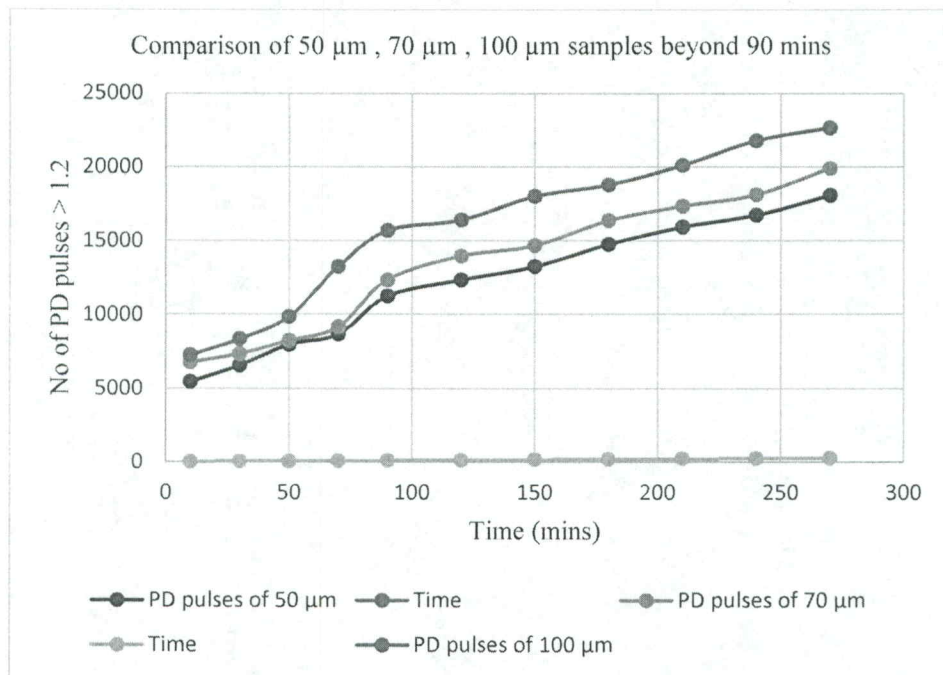
Figure 3.14: Comparison of Passed Samples

From the above plot, it is observed that the PD activity gradually increases over time. As the applied peak-to-peak voltage is constant at 2.5 kV, the electric field within the discharge sites

is not very high and the sample can endure for longer times than the samples at a voltage of 3.2 – 4 kV. These samples also tend to failure but after longer time which is 3 times more than the samples at 3.2kV. It can be inferred that the number of PDs and the PD amplitudes represent the total energy delivered to the insulation by the PD, which is related to the failure of the insulation. Comparison of failed and passed samples is presented below.

3.3.3   Comparison of Failed and Passed Samples

50 μm sample
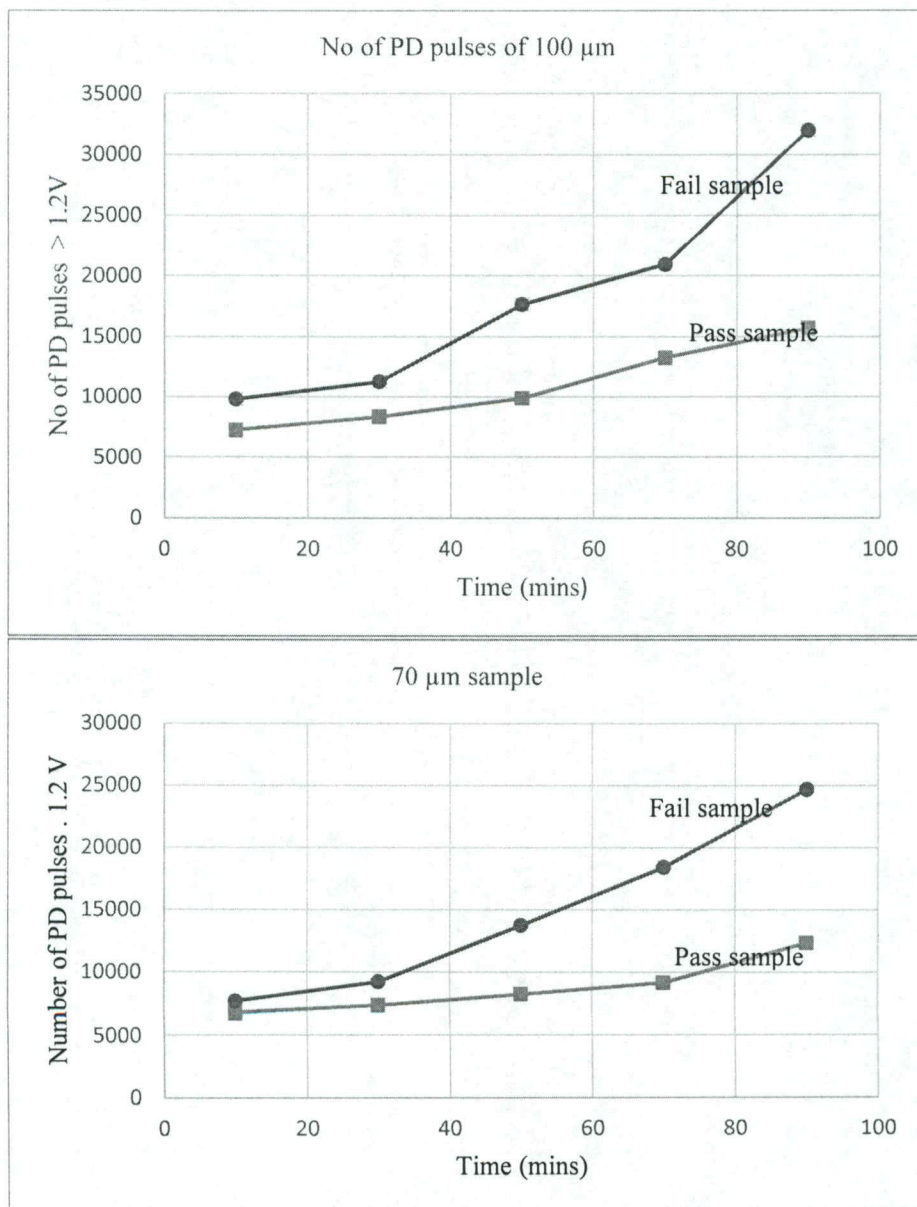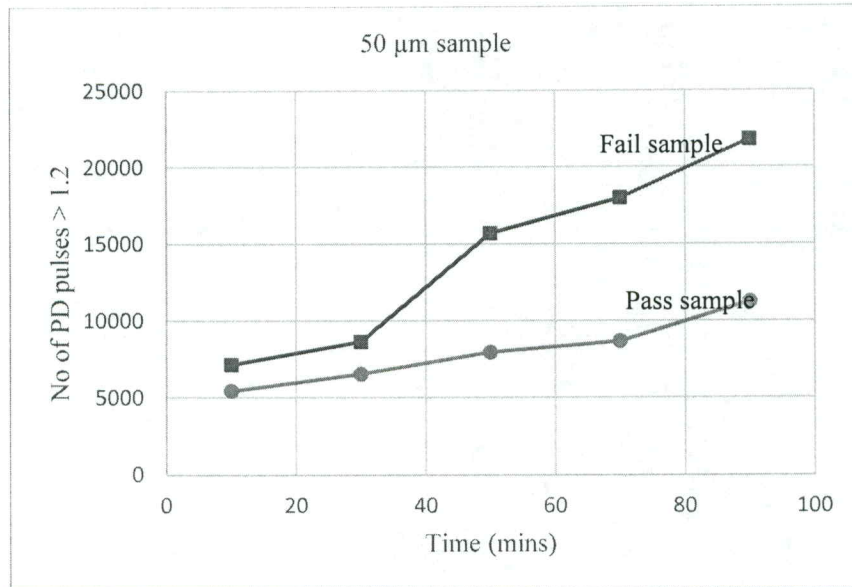
Figure 3.13: Comparison of Failed and Passed Samples of Different Thickness

There is some extra electric field generated by space charges at the discharge area which made samples to fail. Once PD is developed, there will be space charges at that discharge surface, and as the voltage is high, the starting electrons are having more velocity and more collisions which may result in extra discharges. When a discharge happens, there is an accumulation of charge both in the insulation bulk and on the insulation surface. The modification of electric field in the air gap of twisted pair enamel wires due to this space charge accumulation must be studied.

CHAPTER 4

SPACE CHARGE BEHAVIOR AND ELECTRIC FIELD

MEASUREMENT

Overview of a PD Process Happening Inside the Insulation Bulk

Two conditions should be fulfilled so that PD would occur. Firstly, the electric field in the insulation bulk should be high enough. It means that total voltage in a void within insulation bulk should be larger than minimum breakdown voltage V_{min} (PDIV) so that self-sustaining discharge could last. Secondly, starting electron should be present at a suitable position in the void to initiate the ionization process [34]. The statistical time lag t_L determines the appearance of starting electron. Voltage in the void during the time lag may exceed V_{min} by an overvoltage ΔV, and PD ignites at a voltage $V_i = V_{min} + \Delta V$. After a discharge, the voltage across the void drops to the residual value V_{res}. For the next discharge, the voltage across the void needs to again exceed V_{min} in the recovery time t_R. Here V_{min} can be considered as PDIV. In Figure 4.1 voltage variation is depicted to show how the pulse voltage stresses the insulation influencing PDIV.
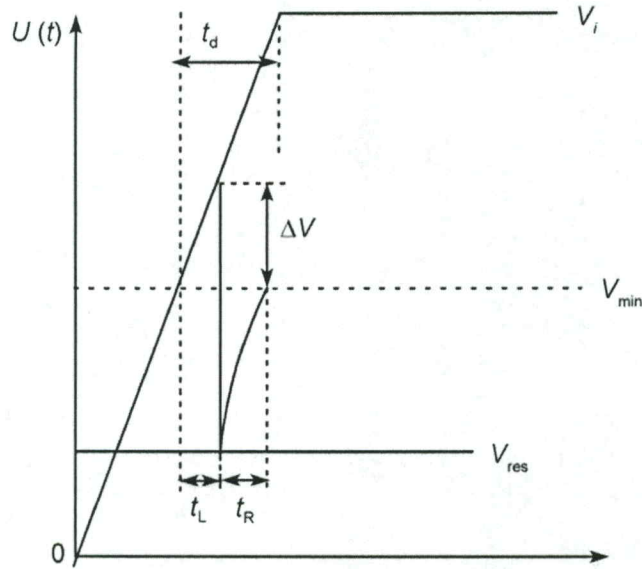
Figure 4.1: Voltage Variation Across a Void in the Insulation Bulk

t_d = total discharge time

t_L = statistical time lag

t_R = recovery time

V_{res} = residual voltage across void after

V_{min} = PDIV of the void within the insulation bulk

V_i = applied voltage

The influence of space charge accumulated within the insulation bulk and on the surface of enamel wires on the electric field within the air gap is investigated. From past literature [5],[6],[7], we understand that Partial Discharge mainly depends on PDIV, PD repetition rate, and PD amplitude. Our goal is to find the factor which is responsible for the decrease in the lifetime of the insulation. From the previous literature [24], space charge accumulation has been considered as the crucial factor affecting the electric field in the air gap of the twisted pair enamel wires. We must determine how this change in the electric field affects PDIV, PD

45

repetition rate and in turn affect the lifetime of the insulation. To find how electric field varies within insulation bulk, a space charge model was assumed.

Twisted pair

Fig 4.2 Twisted Pair Enamel Wires

Above picture shows twisted pair enamel wire and a capacitor model has been assumed from one single turn. The following terms are studied carefully in this section.

- Space Charge Behavior: Enameled wires seem to accumulate charge under DC and with unipolar waveforms even at high frequency, while under bipolar waveforms space charge accumulation becomes negligible with increasing frequency [42].

- Partial Discharge Behaviour: From chapter 3, we have found that PDIV is almost independent of frequency. We must study how PDIV varies with space charge accumulation.

- Life Behaviour: Peak-to-peak voltage, as well as the frequency, is the main factor accelerating aging of the twisted pair enamel samples.

4.1   Electric Field Measurement and Space Charge Model

The electric field in the air gap after a PD event depends on two quantities. One is relevant to the external electric field, and the other is space charge electric field which in turn depends on space charge density left on the insulation surface by the previous PD.

Let us consider the model shown below.
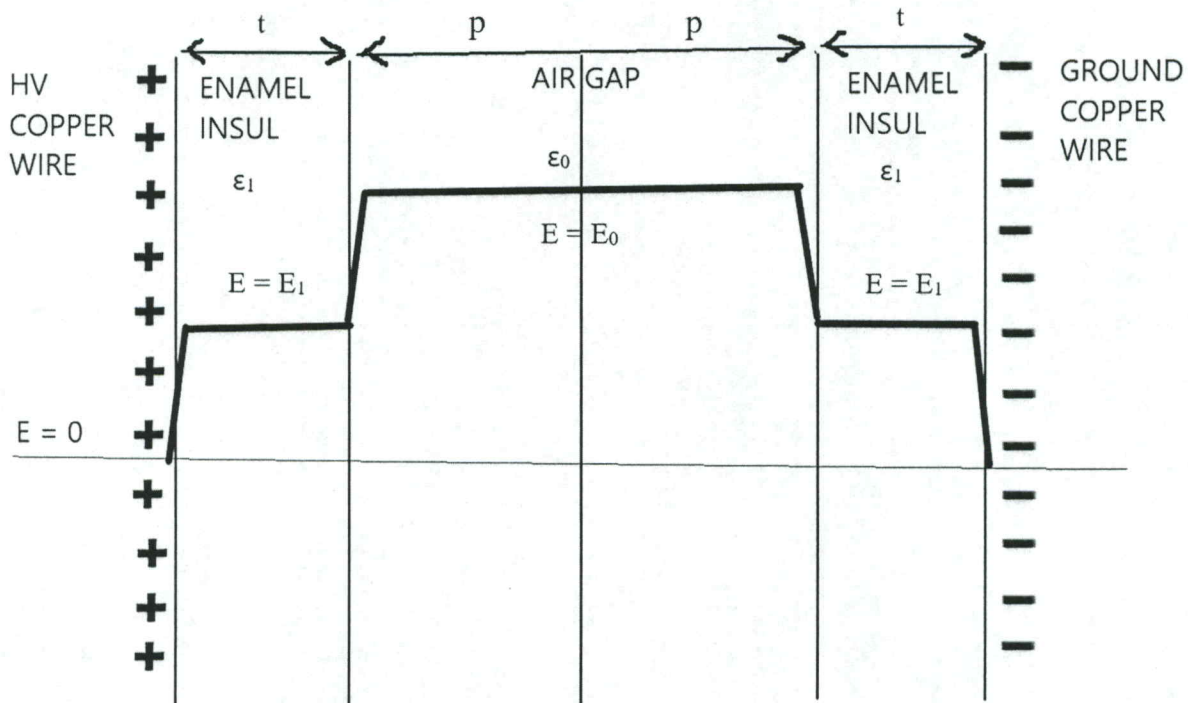
Figure 4.3: Electric Field Variation Across the Air Gap

It is emphasized that PD activity depends on the electric field in the air gap between two enameled wire surfaces such as between the adjacent wires of a twisted pair turn [42]. Theoretical proof of that electric field variation within the air gap can be beneficial for further

analysis of PD behavior. The figure above shows the electric field distribution between plates of a parallel capacitor with mixed dielectrics. We can find the electric field in the air gap. Considering the system symmetrical with respect to the axis passing from the middle of the air gap, there are two cases:

i). Accumulation of space charge in the insulation bulk.

ii). Accumulation of space charge on air/insulation interface.

The electric field (E) between the capacitor plates separated by a distance 'd,' and an applied voltage of 'V' is given by

$$E = \frac{V}{d} = \frac{\sigma}{\varepsilon}$$

Where σ = charge density

ε = permittivity

As shown in the figure we have mixed dielectrics namely enamel insulation of thickness 't' and half the distance 'p' of the air gap as insulation. Let us assume there is **no accumulation of charge** either in the insulation bulk or in the air gap. Now the electric field E_0 can be calculated by the following expression

$$E_0 = \frac{V}{\frac{\varepsilon_0}{\varepsilon_1}t + p} \ldots\ldots\ldots\ldots\ldots\ldots\ldots (1)$$

where p = half of the distance of the air gap

t = thickness of enamel insulation

ε_0 = dielectric constant of air

$$\varepsilon_1 = \text{dielectric constant of enamel insulation}$$

It is evident that, $\varepsilon_1 > \varepsilon_0$ and $E_0 = \frac{\varepsilon_1}{\varepsilon_0} E_1$, where E_1 is the electric field inside the insulation

bulk and then $E_0 > E_1$ and bold line in Figure 4.3 above indicates the electric field in that region.

Our previous researchers have emphasized the fact that space charge accumulation can occur both in the insulation bulk and on the insulation air gap surface [30] and the electric field is getting distorted according to the equation (1). Indicating with $\dot{\rho}$ and σ_s the charge per volume unit in insulation bulk and the charge per surface unit on the interface respectively, then the electric field E becomes E^* in Figure 4.4. The thickness (α) of the charge distribution in insulation bulk is negligible when compared to the thickness of the insulation. Now a relationship can be drawn between the electric field in the right and the left side of the charge distribution namely E_1^* and E_2^* shown in Figure 4.4.
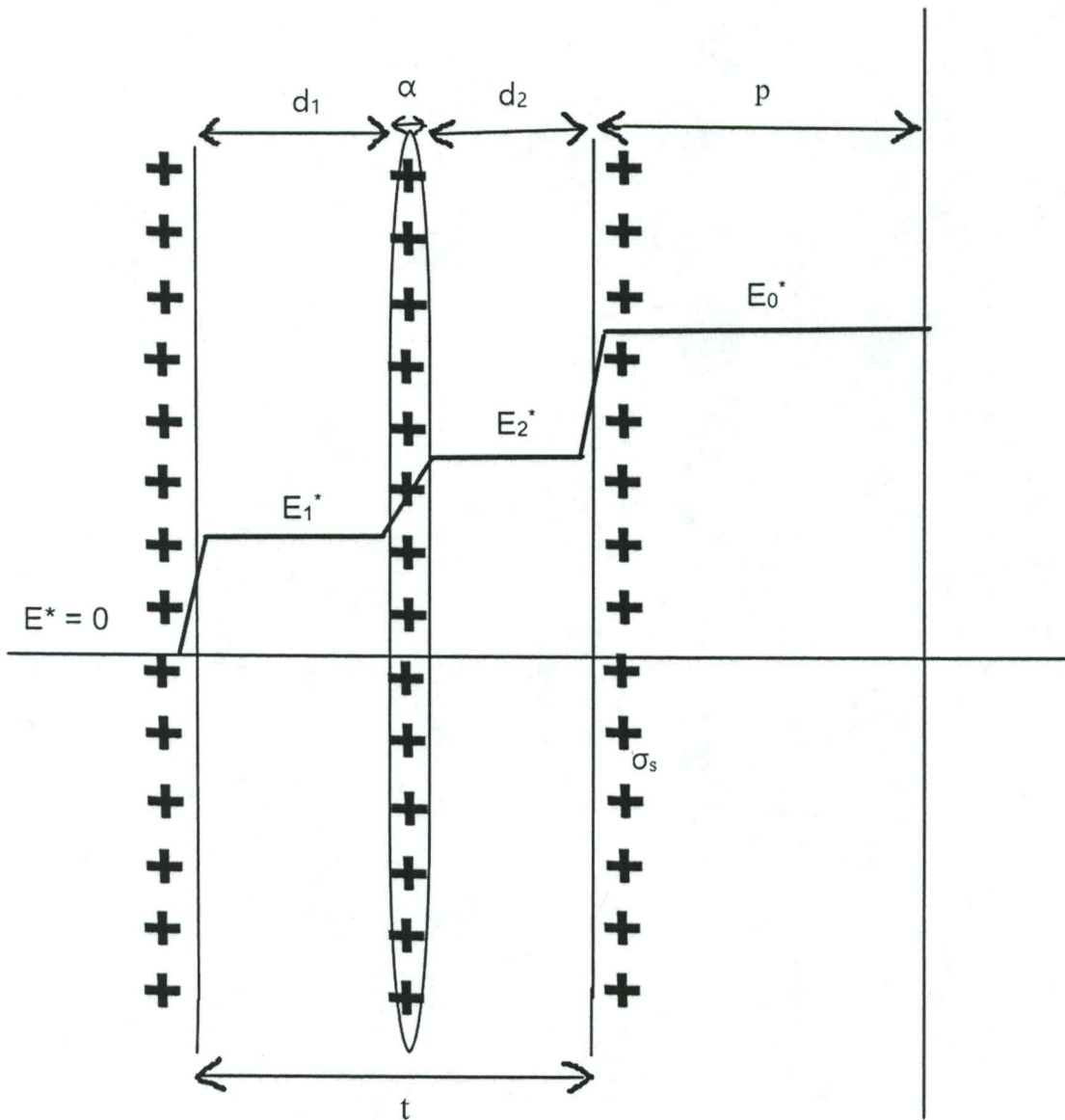
Figure 4.4: Electric Field Variation with Charge Accumulation Both on Air Gap Interface and in the Insulation Bulk

$$E_2^* = E_1^* + \frac{\dot\rho\alpha}{\varepsilon_1} \quad [42] \qquad \text{where } \dot\rho = \text{charge per volume unit in insulation bulk}$$

The electric field in the air gap, E_0^* is related to the charge accumulated on the interface by the following equation [42]

$$E_0^* = \frac{\varepsilon_1}{\varepsilon_0} E_2^* + \frac{\sigma_s}{\varepsilon_0} \quad \text{where } \sigma_s = \text{charge per surface unit on the interface}$$

Consider the system symmetrical with respect to an axis located in the middle of air gap we can observe that

$$E_1^* d_1 + E_2^* d_2 + E_0^* p = V$$

From equation (1), we can deduce the E_0^*

$$E_0^* = E_0 + \frac{\dot{p}\alpha d_1 + \sigma_s t}{\varepsilon_0 t + \varepsilon_1 p} \dotfill (2)$$

Where E_0 is the previous electric field in the air gap in the absence of charge accumulation ($\sigma_s = 0$ and $\dot{p} = 0$).

The electric field generated by space charge both in the insulation bulk and on the surface of the insulation is given by

$$E_{SC} = \frac{\dot{p}\alpha d_1 + \sigma_s t}{\varepsilon_0 t + \varepsilon_1 p}$$

As for unipolar is considered, $\dot{p} > 0$ and $\sigma_s > 0$, that means charge have the same polarity as that of the positive electrode, and $E_0 > 0$. Then from the equation (2) we can assess that there is an increase in the electric field in the air gap due to space charge accumulation. Therefore, the resulting electric field E_0^* is magnified by E_{SC}. To understand the impact of accumulated surface charge on PD characteristics, the space charge effect on PDIV must be investigated.

4.2   Effect of space charge accumulation on PDIV

From equation

$$E_0{}^* = E_0 + \frac{\dot{\rho}\alpha d_1 + \sigma_s t}{\varepsilon_0 t + \varepsilon_1 p} \ldots\ldots\ldots\ldots\ldots\ldots (2)$$

Let us consider charge accumulation inside the insulation bulk, $\dot{\rho} = 0$, and this is only true in the case of perfectly homogeneous dielectrics. So, the charge is present only on insulation surface.

$$E_0{}^* = E_0 + \frac{\sigma_s t}{\varepsilon_0 t + \varepsilon_1 p} \ldots\ldots\ldots\ldots\ldots\ldots (3)$$

In equation (3), this is the field generated by space charge (E_{SC})

$$E_{SC} = \frac{\sigma_s t}{\varepsilon_0 t + \varepsilon_1 p} \text{ (when charge accumulation inside the insulation bulk, } \dot{\rho} = 0)$$

Here ε_0 and ε_1 are the dielectric constants relevant to air and enamel insulation respectively. The charge σ_s is accumulated between the interface of two dielectrics; charge trapping can occur. This charge trapping is related to both conductivity and dielectric induction of the dielectrics.

According to a research paper [42], the interfacial charge density is given by the equation shown below.

$$\sigma_s = E_0{}^* \left(\varepsilon_0 - \varepsilon_1 \frac{\gamma_0}{\gamma_1} \right) \ldots\ldots\ldots\ldots\ldots\ldots\ldots (4)$$

where γ_0 = electrical conductivity of air

γ_1 = electrical conductivity of enamel insulation

Substituting equation (4) into equation (3) we have

$$E_0^* = \frac{E_0}{1 - \frac{\varepsilon_0 - \varepsilon_1 \frac{\gamma_0}{\gamma_1}}{\varepsilon_0 + \varepsilon_1 \frac{p}{t}}} \quad \dots\dots\dots\dots\dots\dots\dots \quad (5)$$

Usually $\varepsilon > \varepsilon_0$ and $\gamma_0 > \gamma_1$ we get $\varepsilon_0 - \varepsilon_1 \frac{\gamma_0}{\gamma_1} < 0$, i.e. $\sigma_s < 0$, which implies σ_s has negative sign with respect to E_0^*. Therefore, interfacial charge favors reducing the electric field in the air gap according to the equation (5) and as a consequence partial discharge inception voltage (PDIV) increases. This is how PDIV varies with space charge accumulation.

It is known that PD is an internal activity within insulation bulk and charge accumulates in the insulation bulk, when supply waveforms have a DC component [32], as it occurs for unipolar waveforms. In some materials charge is mainly injected by the electrodes, so that accumulated charge has the same polarity that of the injecting electrode, e.g., $\dot{\rho} > 0$ for the positive electrode. According to the equation (2), this leads to an increase of electric field in the air gap between two wires and thus to a PDIV decrease.

$$E_0^* = E_0 + \frac{\dot{\rho}\alpha d_1 + \sigma_s t}{\varepsilon_0 t + \varepsilon_1 p} \quad \dots\dots\dots\dots\dots \quad (2)$$

If $\dot{\rho} > 0$ for the positive electrode, E_0^* is increased.

Therefore, interfacial charge and the charge accumulation in the insulation bulk contradict each other, i.e., interfacial charge decreases the electric field in the air gap and the latter increasing electric field in the air gap. They have a cumulative effect on PDIV and breakdown of the insulation.

The extra energy which made the samples to breakdown is the electric field generated due to space charge accumulation within the insulation bulk and on the surface of the insulation.

4.3 Relation Between PDIV, Life Time of the Insulation and Electric Field

The electric field variation in the air gap and in the insulation bulk was investigated based on a theoretical approach. PDIV is dependent on electric field and electric field in turn dependent on the applied peak to peak voltage (V_{P-P}). This electric field is distorted due to accumulated space charge and PDIV varies according to the electric field variation as shown above. Life time of the insulation is dependent directly on peak-to peak voltage of the pulse. In fact, the electric field and PDIV variation are defining the insulation life of the sample. PD activity increases with increase in V_{P-P}. This explains why some of the samples which has high discharge numbers failed early compared to other samples. It can be inferred that the number of PDs and the PD amplitudes represent the total energy delivered to the insulation by the PD, which is related to the failure of the insulation.

CHAPTER 5

CONCLUSION AND FUTURE WORK

5.1   Conclusion

In this thesis, characteristics of partial discharges in the insulated twisted pair wires are analyzed, and the related literature was reviewed. The primary objective of this work is to determine factors which affect the lifetime of the insulated enamel wires employed in the inverter-fed motor windings and to prevent the premature insulation failure of the motors. This is accomplished by investigating the failure mechanism of the enamel wire windings considering twisted pair enamel wire as equipment under test. The dependence of PD characteristics of enamel wire on various parameters of the square wave namely rise time, frequency, pulse width was analyzed. The following conclusions are drawn:

1. The time to breakdown of the sample increases with an increase in rise time. From experimental results, it can be observed that shorter rise times gave rise to PD events of higher magnitude and high inception voltage. For same peak-to-peak voltages, PD repetition rate increases when increasing rise time. Only one PD event is observed when rise time is between 300 ns – 1 µs and multiple (3-4) PD events are found when rise time is longer than 1 µs.

2. The time to breakdown of the sample decreases with increase in frequency. From experimental results, it can be observed that PD magnitude and repetition rate increase with an increase in frequency. This can be attributed to the fact that, with an increase in frequency, the time period of the waveform decreases. Therefore, less time available for the electrons to recombine, generating more free electrons leading to increase in discharges and hence increase in PD. So, the probability of breakdown is high with an increase in frequency.

3. The time to breakdown of the sample decreases with an increase in pulse width. This can be attributed to the fact that when the duty cycle is more, i.e., ON time of the pulse is more, which means voltage is high for the extended amount of time, so there is a more chance of PD occurrence. So, with increasing duty cycle PD increases, which decreases the time to BD of the sample.

4. The partial discharge patterns of samples of different insulation thickness are presented. By analyzing these patterns, the point at which the insulation system is going to break down can be known, and we can take necessary steps to prevent premature insulation failure of the system and thereby evading complete blackout of the motor inverter setup.

5. The number of PD events occurred inside the sample increased as the sample approached to break down. A space charge model has been proposed to understand the PD mechanism behind the above-explained behavior of the twisted pair enamel samples.

6. The effect of space charge accumulation on the modification of the electric field in the air gap between the enamel wires has been investigated. It is explained how PDIV varies with space charge accumulation in the air gap and in the insulation bulk. It has been observed that interfacial charge and the charge accumulation in the insulation bulk

contradict each other, i.e., interfacial charge decreases electric field in the air gap and the latter increasing electric field in the air gap. They have a cumulative effect on PDIV and ultimately the breakdown of the insulation.

5.2 Future Work

- The development of an enameled wire that can withstand coil winding stresses and increase the insulation lifetime of inverter-fed motors is necessary. To extend the withstand voltage life of a motor, its magnet wire must prevent the generation of partial charge even when high-frequency and high voltage are applied.

- The desired characteristics of enamel wire are: the draining of accumulated space charge within insulation bulk, high tolerance for surges and low dielectric permittivity. Therefore, the use of PD-resistant enamel insulation is usually the priority among all other measures.

- A comparison of different insulation materials at the same applied voltage was conducted in the present research. The life endurance of materials at the same electric field level could also be compared, but there are challenges that need to be addressed in doing so, such as variations in thickness from one sample to another.

- Findings confirmed that the PD is the main factor in the aging of insulation and it arises from defects or voids in the insulation system. Future research efforts could conduct investigations on the materials and construction of insulation systems in order to minimize the possibility of defect formation or decrease the vulnerability of the insulation to PD activities. The study on enhancement of the properties of VPI epoxy or the use of nano-filled enamel insulation are some examples.

REFERENCES

[1]   G.G. Gao, M. Steinhauser, and K. Kavanaugh, "Studies on the insulation life of ASD-fed motors under accelerated aging conditions," Pmc IEEE Cov&retzce on Ele&cal Inridation MD Dielectric Phenomna, Austin TX, Oct. 1999, pp. 58 1-584

[2]   H.A. Toliyat et al., "Estimation of voltage distribution on the inverter-fed random wound induction motor windings supplied through feeder cable," 1 Jim, pp. 976-982, Dec. 1999.

[3]   G.C.Montanari, Paolo Seri, Fabrizio Negri, "Partial Discharge And Aging Phenomena In Insulation Systems Of Rotating Machines Fed By Power Electronics" Conference Proceedings of ISEIM 2017, 11-15 Sept. 2017.

[4]   J. C. G. Wheeler, "Effects of converter pulses on the electrical insulation in low and medium voltage motors," IEEE Elect. Insul. Mag., vol. 21, no. 2, pp. 22-29, April 2005.

[5]   M. Kaufhold, G. Borner, M. Eberhardt, and J. Speck, "Failure mechanism of the interturn insulation of low voltage electric machines fed by pulse controlled inverters," IEEE Electrical Insulation Magazine, vol. 12, no.5, pp. 9-16, September-October 1996.

[6]   G.C. Montanari, F. Negri, F. Ciani, "Partial discharge and life behavior of rotating machine wire insulation under PWM waveforms: the influence of inverter characteristics," IEEE EIC, Baltimore, USA, June 2017.

[7]   P. Wang, A. Cavallini, G.C. Montanari, "The influence of repetitive square wave voltage parameters on enameled wire endurance," IEEE Trans. on Diel. El. Ins., Vol. 21, n. 3, pp. 1276-1284, 2014.

[8]   P. Wang, A. Cavallini, G.C. Montanari, "Effect of rise time on PD pulse features under repetitive square wave voltages," IEEE Trans. on Diel.El. Ins., Vol. 20, n.1, pp. 245-254, 2013.

[9]   A. Cavallini, D. Fabiani, and G. C. Montanari, "A novel method to diagnose PWM-fed induction motors," IEEE Trans. on Diel. El. Ins., Vol. 15, n. 5, pp. 1313-1321, October 2008

[10]   G.C. Montanari, "The time behavior of partial discharges and life of type II turn insulation specimens under repetitive impulse and sinusoidal waveforms," IEEE El. Ins. Mag., to be published in 2017.

[11]   IEC TS 60034-18-42:2008, Qualification and acceptance tests for partial discharge resistant electrical insulation systems (Type II) used in rotating electrical machines fed from voltage converters.

[12]   G.C. Stone et al., "Progress in On-Line Measurement of PD in Motors Fed by Voltage Source PWM Drives," *IEEE Electrical Insulation Conference Record*, June 2014, pp 172-175.

[13]   D. Fabiani and G. C. Montanari, "The effect of voltage distortion on aging acceleration of insulation systems under partial discharge activity," IEEE Electrical Insulation Magazine, vol. 17, no. 3, pp. 24–33, Jun. 2001.

[14]   M. Tozzi, A. Cavallini, G.C. Montanari, "Monitoring Off-line and On-line PD under Impulsive Voltage on Induction Motors. Part I: Standard Procedure", IEEE Electr. Insul. Mag, Vol.26, No.4, July/August 2010.

[15]   N. Hayakawa, I. Inano, Y. Nakamura, and H. Okubo, "Time variation of partial discharge activity leading to the breakdown of magnet wire under repetitive surge voltage application," *IEEE Trans. Dielect. Elect. Insul.*, vol. 15, no. 6, pp. 1701–1706, Dec. 2008.

[16]   M. J. Melfi, "Low-voltage PWM inverter-fed motor insulation issues," IEEE *Trans. Ind. Appl.*, vol. 42, no. 1, pp. 128–133, Feb. 2006.

[17]   G.C.Montanari, Fabio Ciani, "Inverter design and partial discharge phenomenology in insulation systems of rotating machines."

[18]   Rotating Electrical Machines—Part 27-1: Off-Line Partial Discharge Measurements on the Stator Winding Insulation of Rotating Electrical Machines, IEC 60034-27-1, under revision.

[19]   W. T. Starr and H. S. Endicott, "Progressive stress: A new accelerated approach to voltage endurance," *IEEE Trans. Power Appl. Syst.*, pp. 515–522, 1961.

[20]   G. C. Montanari, G. Mazzanti, and L. Simoni, "Progress in electrothermal life modeling of electrical insulation over the last decades," *IEEE Trans.Dielectr. Electr. Insul.*, vol. 9, no. 5, pp. 730–745, 2002.

[21]   G. C. Stone, S. Campbell, and S. Tetreault, "Inverter-fed drives: Which motor stators are at risk?" *IEEE Ind. Appl. Mag.*, vol. 6, no. 5, pp. 17–22,2000.

[22]   G. C. Montanari, "Power electronics and electrical apparatus: A threat?" in *Nordic Insul. Symp.*, 2007, pp. 1–9.

[23]   Basava Raja and D.V.S.S. Siva Sarma. 2006. Modeling and Simulation of dv/dt filters for A.C Drives with fast switching Transients. Power India Conference. IEEE Publication on 10-12 April.

[24] Kaoru Takizawa; Tomoki Suetsugu; Hiroaki Miyake; Yasuhiro Tanaka, " Space charge behavior in covering insulating material for motor windings under applied voltage of square wave" Conference Proceedings of ISEIM 2014

[25] Peng Wang, Andrea Cavallini, Gian Carlo Montanari, "The Effect of Impulsive Voltage   Rise Time on Insulation Endurance of Inverter-fed Motors," IEEE 11th International Conference on the Properties and Applications of Dielectric Materials, 2015.

[26] Peng Wang, Andrea Cavallini, Gian Carlo Montanari, "The effects of Asymmetry Repetitive Square Wave Voltages on PD Statistics and Endurance," IEEE International Conference on Dielectrics, 2016.

[27] Taufik, Erin Matsumoto, Makbul Anwari, "Impact of multiple adjustable speed drive system to power system harmonics," IEEE 2nd International Power and Energy Conference, 2008.

[28] Peng Wang, Andrea Cavallini, Gian Carlo Montanari, "The influence of square wave voltage duty cycle on PD behavior," IEEE Conference on Electrical Insulation and Dielectric Phenomena, 2015.

[29] Peng Wang, Andrea Cavallini, Changjiang Zheng, Ying Li, Yong Lei, "The PD and Endurance Features of Enameled Wires at Short Repetitive Impulse Voltages," IEEE Electrical Insulation Conference (EIC), 2018.

[29] Peng Wang, Jian Wang, Hongying Xu, Kai Zhou, Yong Lei, Qun Zhou, "Comparative study of PD characteristics for inverter-fed motor insulation under sinusoidal and repetitive square wave voltage conditions," IEEE International Conference on High Voltage Engineering and Application (ICHVE), 2016.

[31] Tomoyuki Iwata, Takaya Momose, Hiroaki Miyake, Yasuhiro Tanaka, "Measurement of space charge distribution in coating material for motor windings under square wave voltage," IEEE International Conference on Dielectrics (ICD), 2016.

[32] Koichi Ota, Kensuke Kumaoka, Takashi Saiki, Hiroaki Miyake, Yasuhiro Tanak, "Space charge distribution measurement in corona discharged filler added polyimide films under DC stresses," IEEE International Conference on Dielectrics (ICD), 2016.

[33]   Peng Wang, Andrea Cavallini, Gian Carlo Montanari, "The influence of impulsive voltage frequency on PD features in turn insulation of inverter-fed motors," IEEE Conference on Electrical Insulation and Dielectric Phenomenon (ICEIDP), 2014.

[34]   Kai Zhou, Guangning Wu, "Partial Discharge activity of interturn insulation under different parameters of square wave voltage," IEEJ Transactions on Fundamentals and Materials, 2009.

[35]   Gian Carlo Montanari, Fabio Ciani, "Partial discharge and life behavior of rotating machine wire insulation under PWM waveforms: the influence of inverter characteristics," Electrical Insulation conference,11-14 2017.

[36]   N. Hayakawa, H. Inano, K. Inuzuka, M. Morikawa, H. Okubo, "Partial Discharge Propagation and degradation characteristics of magnet wire for Inverter-fed motor under surge voltage application," Annual report Conference on Electrical Insulation and Dielectric Phenomena, 2006.

[37]   N. Hayakawa, H. Inano, K. Inuzuka, M. Hamaguchi, H. Okubo, T. Hirose, "Partial Discharge characteristics of Nanocomposite enameled wire for inverter-fed motor," Annual report conference on Electrical Insulation and Dielectric Phenomena, 2006.

[38]   N. Hayakawa, H. Inano, K. Inuzuka, M. Hamaguchi, H. Okubo, T. Hirose, "Lifetime Characteristics of Nanocomposite Enameled Wire under Surge Voltage Application," Annual report Conference on Electrical Insulation and Dielectric Phenomena, 2007.

[39]   Kei Ooi, Masafumi Yashima, and Tatsuki Okamoto, "Investigation of Partial Discharge Life Characteristics of Twisted Pair of Enamelled wires," Conference proceedings of ISEIM, 2017.

[40]   Investigation of Partial Discharge Occurrence and Detectability in High Voltage Power Cable Accessories by Jarot Setyawan, Graduation Thesis.

[41]   L. R. Zhou, G. N. Wu, B. Gao, K. Zhou, J. Liu, K. J. Cao, L. J. Zhou, "Study on charge transport mechanism and space charge characteristics of Polyimide films", IEEE Transactions on Dielectrics and Electrical Insulation, Vol. 16, No. 4; August 2009.

[42]   D. Fabiani, G. C. Montanari, A. Cavallini, G. Mazzanti, "Relation between space charge accumulation and Partial discharge activity in enameled wires under PWM like voltage waveforms," IEEE Transactions on Dielectrics and Electrical Insulation, Vol. 11, No.3; 2004.

[43]   D. Fabiani, A. Cavallini, G. Mavanti and G. C. Montanari, "The effect of charge mobility on Partial discharge characteristics of enameled wires for PWM controlled motors," 2004 International Conference on Solid Dielectrics, 2004.

[44]   X. Wang, C. Chen, J. Z. Xiong, Kai Wu, D.M. Tu, "Formation mechanism of space charge in silicone rubber insulation under low DC stress," IEEE International Conference on the Properties and Application of Dielectric Materials (ICPADM), 2015.

[45]   Gian Carlo Montanari, Paolo Seri, Fabrizio Negri, "Partial Discharge And Aging phenomena In Insulation Systems of Rotating Machines Fed By Power Electronics," Conference Proceeding of ISEIM, 2017.

[46]   Jeffrey C. Chan, Hui Ma, Tapan K. Saha, "Time-frequency Sparsity Map on Automatic Partial Discharges Sources Separation for Power Transformer Condition Assessment" IEEE Transaction on Dielectrics and Electrical Insulation, Vol. 22, No. 4, 2015.

[47]   Lu Cui, Weigen Chen, A. S. Vaughan, Bo Xie, Jian Li, Zhenze Long, "Comparative Analysis of Air-gap PD characteristics: Vegetable Oil/pressboard and Mineral Oil/pressboard," IEEE Transactions on Dielectrics and Electrical Insulation, Vol. 24, No. 1; 2017.

[48]   J. Benzing, C. L. Patterson, B. J. Cassidy, I. Blokhintsev, A. H. Loesch, "Continuous online partial discharge monitoring of medium voltage substations", IEEE IAS/PCA Cement Industry Conference, 2012.

[49]   Handbook on Insulation Materials Selection and Installation

[50]   A thesis by Angelo J. Ballungay, "High voltage pulse measurement system," 2013.

[51] J. C. G. Wheeler, "Effects of converter pulses on the electrical insulation in low and medium voltage motors," IEEE Electr. Insul. Mag., vol. 21, no. 2, pp. 22–29, 2005.

[52]   "Available at website: http://www.eetimes.com/."